



Orally-delivered insulin-peptide nanocomplexes enhance transcytosis from cellular depots and improve diabetic blood glucose control

Sahrish Rehmani^a, Christopher M. McLaughlin^b, Hoda M. Eltaher^a, R. Charlotte Moffett^b, Peter R. Flatt^b, James E. Dixon^{a,*}

^a Regenerative Medicine & Cellular Therapies, The University of Nottingham Biodiscovery Institute (BDI), School of Pharmacy, University of Nottingham, Nottingham NG7 2RD, UK

^b Diabetes Research Centre, School of Biomedical Sciences, Ulster University, Coleraine, Co. Londonderry BT52 1SA, UK

ARTICLE INFO

Keywords:

Oral insulin delivery
Glycosaminoglycan-GAG-binding enhanced transduction (GET)
Cell penetrating peptides (CPPs)
Trans epithelial delivery
Transcytosis

ABSTRACT

Insulin regulates blood glucose levels, and is the mainstay for the treatment of type-1 diabetes and type-2 when other drugs provide inadequate control. Therefore, effective oral Insulin delivery would be a significant advance in drug delivery. Herein, we report the use of the modified cell penetrating peptide (CPP) platform, Glycosaminoglycan-(GAG)-binding-enhanced-transduction (GET), as an efficacious transepithelial delivery vector *in vitro* and to mediate oral Insulin activity in diabetic animals. Insulin can be conjugated with GET *via* electrostatic interaction to form nanocomplexes (Insulin GET-NCs). These NCs (size and charge; 140 nm, +27.10 mV) greatly enhanced Insulin transport in differentiated *in vitro* intestinal epithelium models (Caco2 assays; >22-fold increased translocation) with progressive and significant apical and basal release of up-taken Insulin. Delivery resulted in intracellular accumulation of NCs, enabling cells to act as depots for subsequent sustained release without affecting viability and barrier integrity. Importantly Insulin GET-NCs have enhanced proteolytic stability, and retained significant Insulin biological activity (exploiting Insulin-responsive reporter assays). Our study culminates in demonstrating oral delivery of Insulin GET-NCs which can control elevated blood-glucose levels in streptozotocin (STZ)-induced diabetic mice over several days with serial dosing. As GET promotes Insulin absorption, transcytosis and intracellular release, along with *in vivo* function, our simplistic complexation platform could allow effective bioavailability of other oral peptide therapeutics and help transform the treatment of diabetes.

1. Introduction

Therapeutic proteins differ in their size, charge, and structure; all these features having influence on complex formation between delivery agent and the protein of interest. Effective delivery of therapeutic proteins using carriers depends on several factors such as; a) type of linkage (hydrophobic or electrostatic interaction), b) optimal protein/carrier concentration and volumes, c) minimal cell toxicity, d) complex internalization and protein/carrier release [1,2]. Insulin, a hormone and important blood glucose-lowering therapeutic peptide, is secreted by pancreatic β -cells. To date, Insulin formulations are only approved for administration by the subcutaneous, nasal or pulmonary routes; however, application through the oral route continues to be the most clinically attractive but has evaded success over more than two decades.

Multiple formulations for oral Insulin administration have entered clinical trials, ranging from simple enteric-coated capsules, liposomes, polymer conjugates, and formulations with absorption/permeation enhancers to buccal sprays [3,4]. Peptides that act as protein transduction domains (PTDs), cell penetrating peptides (CPPs) or membrane translocating sequences (MTSS) have been exploited for a variety of delivery challenges (*e.g.* for protein, nucleic acid, and other diagnostic/therapeutic drug molecule delivery) [5] including experimental Insulin formulations [6–19]. CPPs can effectively deliver therapeutic proteins ranging in size from 30 kDa (*e.g.*, GFP) to 120–150 kDa (*e.g.*, antibodies IgG) and the most advanced multi-functional delivery systems possess minimal immunogenicity, improved stability, amenable chemical versatility and controllable release to allow specific drug delivery [20–25]. Several early studies have investigated the potential of variety

* Corresponding author at: Regenerative Medicine & Cellular Therapies, The University of Nottingham Biodiscovery Institute (BDI), School of Pharmacy, University Park, University of Nottingham, Nottingham NG7 2RD, UK.

E-mail address: james.dixon@nottingham.ac.uk (J.E. Dixon).

<https://doi.org/10.1016/j.jconrel.2023.06.006>

Received 16 January 2023; Received in revised form 23 May 2023; Accepted 4 June 2023

Available online 22 June 2023

0168-3659/© 2023 The Authors. Published by Elsevier B.V. This is an open access article under the CC BY license (<http://creativecommons.org/licenses/by/4.0/>).

of CPPs in improving the poor permeability of Insulin across intestinal mucosal membranes. Recent discoveries confirm that low permeability may be improved either by direct conjugation or through electrostatic coupling to form stable nano- or micro-complexes (NCs or MCs). Morishita et al., demonstrated the potential of CPPs octa-arginine and Penetratin to significantly increase intestinal and nasal Insulin absorption following administration as simple mixtures [26,27]. An improved understanding of the transport mechanisms and membrane interactions of novel delivery systems may result in further refinement to achieve the bioavailability required for an effective oral Insulin formulation [10,28–31].

We have described a CPP-based system termed Glycosaminoglycan (GAG)-binding enhanced transduction (GET) [10]. This technology exploits enhanced membrane-docking peptides which bind heparan sulfate glycosaminoglycans (GAGs), combined with CPPs. The prototypical GET peptide fuses the GAG-/heparan sulphate (HS) binding domain P21 (P), derived from heparin-binding epidermal growth factor (HB-EGF) with octa-arginine 8R (R), a CPP, and endosomal escaping peptide, LK15 (L), and was termed P21-LK15-8R (PLR) as a single synthesized peptide [10]. GET is effective in enhancing intracellular transduction of nucleic acids (such as plasmid(p) DNA, siRNAs, modified nucleotide mRNA) [13,15–17], recombinant proteins [6,7] and peptides [19]. GET has also been exploited for spatio-temporal cell programming [12], controlled release [6,7,13], magnetically targeted therapies [8,9,14], for enhanced gene delivery to lungs [15], and for regenerative medicine [11,16,17]. To date, the GET system has not been assessed for its potential to deliver peptide hormones such as Insulin.

Here in, we developed GET-mediated Insulin formulations for oral delivery, termed Insulin-GET nanocomplexes (NCs). The focus here was Insulin delivery, however it could be considered a model for other peptides that could be employed with GET. We employed assays to assess complexation, stability, uptake, and intracellular transduction across *in vitro* intestinal barrier models using differentiated Caco-2 transwell assays. We characterized the interaction and cellular mechanism involved in uptake, that being endocytosis. We assayed complexation of GET/Insulin using fluorescently-labelled Insulin in quenching assays and exploited these for tracking transcytosis and stability. We showed that GET-mediated delivery generates cellular Insulin depots, which are subsequently released, demonstrating cell-based controlled and sustained release of Insulin from delivered cell barriers. We confirm the utility of GET *in vivo* by demonstrating long-term normoglycemia by reduction of blood glucose levels (BGLs) in streptozotocin (STZ)-induced diabetic mice with oral administration. Importantly, GET peptide-based delivery should now be explored as a novel oral therapeutic strategy and combined with delivery systems that will enhance its bioavailability. GET represents the most simple and effective delivery system developed to date, therein showing significant promise for effective Insulin delivery and other peptide therapeutics for treating diabetes by the oral route.

2. Materials and methods

2.1. Materials

A complete list of materials is provided in the supplemental materials section.

2.2. Peptides

All peptides were purchased from Synpeptide (Shanghai, China) at >95% purity. In-house confirmation of peptide purity and molecular weight was carried out by RP-HPLC and MALDI-TOF MS, as previously described [32].

2.3. Cell lines

Human colorectal adenocarcinoma Caco-2 cells (ATCC, HTB-37) were cultured in growth media (GM) as per standard protocols as described previously [10,33]. For delivery experiments, cells were cultured in serum free media (SFM), which was phenol red-free DMEM media supplemented with standard additives except the fetal bovine serum (FBS). Insulin reporter iLite cells (avian DT-40-derived, Product code BM3060; Svar Life Sciences) were used directly from frozen vials. Assays were conducted in RPMI 1640 medium (supplemented with 10% (v/v) FBS, 100 μ M β -mercapto-ethanol, 1% (v/v) chicken serum, 1% (v/v) Penicillin and Streptomycin and 2 mM L-glutamine) as per the manufacturers' instructions.

2.4. Insulin-GET NC formulation

Insulin (Ins) (Sigma, Cat: 91077C, sodium salt, 27.5iU/mg) was labelled with green (FITC, termed Ins-F) and red (TRITC, termed Ins-T) fluorescent dyes using NHS-ester chemistry or purchased (Ins-F*) (Supplemental materials). Insulin variants were mixed with P21-LK15-8R (PLR) peptide (1 mM) (Table S1) in either nuclease-free water (NFW), phosphate-buffered saline (PBS) or SFM (Phenol-red free) in polypropylene tubes. Following addition, the mixture was incubated at room-temperature (RT) for 15 min to form Insulin-GET NCs. Final concentrations of Insulin and PLR in Insulin-GET NC formulations for *in vitro* testing (0.5 ml apical volumes) were typically 20 μ g/ml (10 μ g, 0.275iU) and 10 μ M (27.77 μ g, 55.53 μ g/ml), respectively, unless stated (Insulin:GET, 1:2.7 mass). Testing included ratios of Insulin:GET 20:1 to 1:20 with Insulin concentrations from 0.2 to 200 μ g/ml. For studying permeation and internalization by cell monolayers, transcytosis, and release (during and post-delivery), non-labelled Insulin (Ins), in-house labelled FITC-Insulin (Ins-F, non-quenchable), and TRITC-Insulin (Ins-T) were used. For studying stability of Insulin-GET NCs, FITC-Insulin (Sigma, Cat. No. I3661) (Ins-F*, quenchable) was used.

2.5. Physicochemical complex characterization

The hydro-dynamic diameter and polydispersity index (PDI) of Insulin and Insulin-GET NCs were determined in NFW using quartz cuvette (ZEN2112) by dynamic light scattering (DLS) spectrophotometer equipped with He/Ne laser and 173° detection optics in Malvern Zetasizer (Nano ZS90, UK). Insulin-GET NCs were freshly prepared before analysis. Zeta potential was measured by employing Laser Doppler anemometry. All measurements were carried out in triplicates at 25 °C and each measurement as 10 runs.

2.6. TEM morphological analyses

Morphology and particle size of Insulin and Insulin-GET NCs was further confirmed through TEM (FEI, Tecnai™ G2 12, USA) with an accelerating voltage of 100 kV and 4–6 images were taken per grid. Briefly, a drop of sample (30 μ l) was cast onto a 200 mesh copper grids with carbon film. Excess solution was removed, and grids air-dried. Prior to imaging, grids were stained with heavy metal stain (TAAB EM-336) and dried completely before analysis. Images were acquired at several different magnifications.

2.7. Transepithelial permeation assay

Caco-2 cells were seeded at 2×10^5 cells/well (in GM; 500 μ l apical/top, 1 ml basal/bottom) in transwells (Corning transwell polyester cell culture inserts; Cat. No. 3460, 12 mm diameter transwell inserts with 0.4 μ m pore size) and differentiated for 7 days which was sufficient to form compact monolayers with tight junctions and robust TEER measurements [33]. Media was changed every other day. For delivery, 10 μ g Insulin (unlabelled or labelled versions) was diluted in 25 μ l SFM

(Phenol-red free), mixed, and the correct PLR peptide concentration in 25 μ l SFM added to the diluted Insulin. The resulting solution was mixed and incubated for 15 min at RT to allow complexation. Wells were aspirated, washed with PBS three times and 450 μ l SFM (Phenol-red free) replaced. The prepared formulations (50 μ l) were added and incubated under standard conditions. Media samples (50 μ l) were collected from the basal chamber at 0, 1, 2, 4, 6 and 24 h (h) and the volume removed replaced with SFM. Percentage drug transport/transcytosis and permeability co-efficient (P_{app}) were determined by fluorometry (Tecan infinite 200PRO multimode microplate reader) with excitation (Ex)/emission (Em) of 490 nm/520 nm for FITC-labelled samples as biological and technical triplicates.

2.8. Cell uptake assay by flow cytometry

Caco-2 cells undergoing permeability testing were harvested from transwell inserts after delivery and analysed using a MoFlo Astrios cell sorter (Beckman coulter) (>20,000 events per sample) with blue diode/argon laser (495 nm) to quantify cellular internalization. Flow cytometry results were analysed using WEASEL software and mean fluorescence intensity (MFI) and percentage positivity after gating was used for statistical analysis.

2.9. Transepithelial electrical resistance (TEER) measurement

Monolayer integrity was determined by measuring TEER values before and after formulation delivery using EVOM2 Volt–Ohm–metre (World Precision Instruments, Hitchin, UK) as previously described [33]. Background conductance was removed by subtracting acellular scaffold readings. Electrodes were equilibrated to transwell insert media for 15mins prior to measurements. Following seeding of Caco-2 cells on inserts, TEER was measured daily for the 7 days differentiation to confirm cell growth and establishment of barrier integrity on transwell inserts [33]. TEER readings were taken during and post-delivery and expressed as a percentage of the initial TEER reading (Ω/Ω_0) cm^{-2} .

2.10. Cell metabolism and viability

PrestoBlue® assays (Invitrogen) were conducted to assess effects on cell metabolism as described previously [34]. These are based on resazurin reduction and were normalized to non-delivered controls as full metabolic activity (100%). These assays were performed in 96-well plates or in transwells (0.5 ml top and 1 ml bottom chambers) with incubation time modified (1 h for transwells) to generate a significant signal for fluorometry. Trypan blue exclusion assays and LIVE/DEAD assays were conducted to assess cell viability as described previously [35].

2.11. In vivo studies of blood glucose control

Male HsdOla:TO mice (Envigo, London, UK) at 12-week-old were maintained in an environmentally controlled laboratory at 22 ± 2 °C with a 12 h dark and light cycle with *ad libitum* access to standard rodent diet (10% fat, 30% protein and 60% carbohydrate: Trow Nutrition, Northwich, UK) and drinking water. Induction of diabetes was carried out using Streptozotocin (STZ, Sigma, Dorset, UK) dissolved in sodium citrate buffer (pH 4.5) and promptly administered intraperitoneally at a dose of 160 mg/kg body weight to overnight fasted mice [36]. After administration of the single STZ injection, food was replaced and water supplemented with sucrose (10% w/v), animals were monitored daily thereafter. The onset of hyperglycaemia was measured over the following week with non-fasting blood glucose levels of >20 mmol/l considered appropriate for inclusion within the study. For assessment of bioactivity, human Insulin preparations of 2IU/kg intraperitoneal (IP), or 100–500iU/kg were administered alone or in combination with various ratios of GET (1:5, 1:0.5 and 1:0.05) by oral gavage. Blood

samples were obtained prior to and after administration of assigned treatments from the lateral tail vein of conscious mice at 0 to 240 min. Blood glucose was measured using an Ascencia Contour blood glucose meter (Bayer Healthcare, Newbury, UK). During the AM/PM (morning/evening) dosing study glucose values were measured using a calibrated GOD-PAP assay with a standard curve developed in-house (Glucose GOD-PAP reagent, Randox, UK). All animal experiments were conducted in accordance with the UK Animals (Scientific Procedures) Act 1986 and EU Directive 2010/63EU. All necessary steps were taken to prevent any potential animal suffering. The animal studies were approved by local Ulster Animal Welfare and Ethical Review Body (AWERB) committee.

2.12. Statistical analysis

All experiments were completed as triplicate (technical) and quintuplicate (biological) replicates. Results were expressed as mean values and standard deviation (mean \pm SD). Significance differences were determined using ANOVA (one way- and two-way ANOVA with Bonferroni and Tukey's test, along with determination of normality and distribution of data, and identifying outliers) between the treatments and the respective controls and *p*-value of <0.05 was considered to be significant. Analysis of area under the curve (AUC) were calculated using a trapezoidal rule with baseline subtraction.

3. Results

3.1. Fluorescence quenching can quantitatively determine GET-insulin complexation

We have previously demonstrated that the GET peptide system enhances endocytotic uptake of cargoes electrostatically bound as nano-complexes (NCs). We therefore assessed the ability of PLR peptide to interact with Insulin, with the aim of improving its transepithelial penetration for oral delivery. GET peptides are cationic/positively charged, and cationic CPPs used in other studies have been previously shown to efficiently complex to negatively charged Insulin (pI 5.3) by simple mixing [26,37–40]. Insulin-GET complexes (termed nano-complexes, NCs) were generated by mixing PLR with Insulin. PLR peptide contains the GAG-binding motif P21 (P) which enhances cell surface binding, LK15 (L) an amphiphilic peptide that enhances endosomal escape, and the octa-arginine (8R) CPP (R), which improves endocytosis [10]. We initially developed a fluorescence-based assay for Insulin complexation in which interaction quenched fluorophore-labelled Insulin fluorescence (detailed description in Supplemental section 1.3). The principle is that fluorescence is quenched when several molecules are in close proximity either due to self-association or oligomerization [41]. We hypothesized such phenomenon would give an indication of the stability and intactness of Insulin-GET NCs [42,43]. Two differently labelled Insulin formulations; Ins-F* (a proprietary product with a single fluorescein label) and in-house labelled Insulin (NHS-Fluorescein labelled single lysine side-chain) were evaluated by complexing with different GET peptide concentrations (Fig. 1). Progressive fluorescence quenching is observed for Ins-F* with increasing GET peptide concentration (Table S1). From a 1 μ M concentration of PLR (with 10 μ g Insulin), there is significant quenching with 4 μ M concentration extinguishing all fluorescence to almost blank values. Ins-F is not quenched whatsoever by PLR addition (Fig. 1A). We determined that complexation was practically instantaneous with stable NCs formed within seconds (not shown). Deconstructed GET peptide constituent peptides; P21, LK15 and 8R were tested and although quenching was not complete, the separate peptides (containing P21 and LK15 or 8R) generated >90% reduction of fluorescence (Fig. 1B). Importantly, we confirmed that simple complexation of Insulin and PLR eliminated the need for chemical conjugation and allowed rapid generation of Insulin complexes.

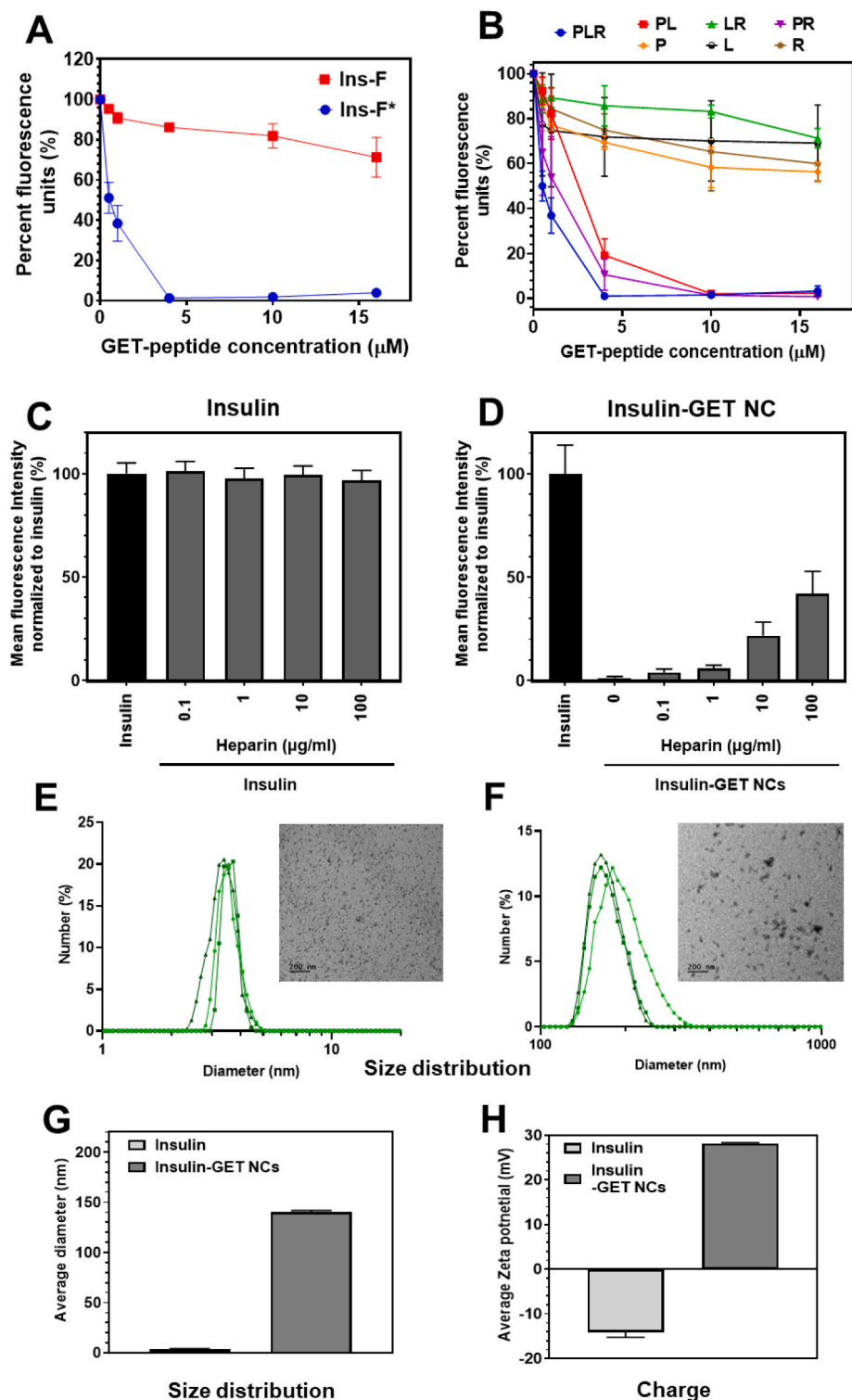


Fig. 1. GET binding to Insulin via electrostatic interaction to form NCs. Quenching of Ins-F and Ins-F* fluorescence with complexation of PLR and component peptides. A. Percent fluorescence quenching of Ins-F and Ins-F* with PLR peptide showing that PLR quenches the fluorescence of Ins-F* almost completely but has little effect on Ins-F. B. PLR, PR, and PL peptides quench the fluorescence of Ins-F* almost completely. C. Percent fluorescence recovery of Ins-F* with Heparin showing no effect on fluorescence. D. Percentage fluorescence recovery of Ins-F* complexed with GET in Insulin-GET NCs showing that GET peptide (PLR) quenching the fluorescence of Ins-F* is partially recovered by increasing Heparin. All values are presented as mean \pm S-D, $n = 5$, * = p -value < 0.05 , ** = p -value < 0.005 , *** = p -value < 0.0005 , **** = p -value < 0.0001 , and ns = not significant. Two-way ANOVA with Tukey's test. Average diameter of particles by DLS measurement for 20 $\mu\text{g/ml}$ of E. Insulin and F. Insulin complexed with GET (10 μM PLR) to form NCs and suspended in water (pH 7) (distribution by number). Inset: Morphology and particle size of Insulin and Insulin-GET NCs was further confirmed through TEM (FEI, Tecnai™ G2 12, USA) with an accelerating voltage of 100 kV. G. DLS analysis for Insulin and Insulin-GET NCs showing size distribution by intensity (avg. diameter). H. Surface charge, where the shift in zeta potential indicates interaction of GET with Insulin to form NCs. ($n = 3$ independent experiments, 10 sub-runs per repeat and values are plotted as mean \pm S-D.).

3.2. Fluorescence recovery from insulin-GET NCs can measure decomplexation and complex stability

We continued characterization of a specific Insulin-GET formulation (1:2.7 mass; Table S1) as a model. Using the quenching assay, we assessed dequenching as a function of Insulin-GET NC stability (Supplemental section 1.3). Initially we employed free or GET complexed Ins-F* with Heparin, which is known to decomplex GET nanoparticles [9] (Fig. 1C,D) and proteolytic enzymes (Proteinase K, PK; Trypsin)

(Fig. S1) which should cleave both Insulin and GET removing fluorescence quenching. As expected, high concentrations of Heparin could partially dequench Insulin-GET NCs (Fig. 1C, D), with no effect on Insulin itself. For proteolytic digestion, exposing free Ins-F* to these enzymes caused further increase in fluorescent intensity, with the hypothesis that the Fluorescein was already partially quenched by conjugation to Insulin (Fig. S1A, B), and proteolytic cleavage released free Fluorescein which was more excitable. PK treatment of Insulin-GET NCs caused rapid recovery of fluorescence of Ins-F*-GET NCs

(fluorescence dequenching), with 40 min digestion recovering the fluorescence values to that of non-complexed Insulin (Fig. S1C, D). With trypsin, there was slower recovery of fluorescence, likely due to the kinetics of the proteolysis, with 180 min required for control values to be achieved (Fig. S1E, F). These results suggest that Insulin-GET NCs can be efficiently cleaved and that by proteolytically disrupting the electrostatic interaction between GET and Insulin can recover fluorescence completely. Additionally, this dequenching phenomenon was time dependent, even with the highest concentration of enzymes tested. To extend our stability analyses we pre-treated PLR peptide with PK (or heat-inactivated PK as a control) and assessed the ability of degraded peptide to complex and quench Insulin. PLR was degraded by active PK, meaning it lost its ability to quench Ins-F* fluorescence, demonstrating that an intact PLR peptide was required for complexation (data not shown).

3.3. Characterization of GET-based insulin NCs

The hydrodynamic diameter and zeta potential of Insulin-GET NCs was measured (at pH 7.0). Insulin alone was relatively monodispersed showing particles of 2.5–5 nm (number distribution), however some larger aggregates of <150 nm and 600–1000 nm size (intensity distribution) were observed which could be removed by low-speed

centrifugation (200 ×g for 5 min) (Polydispersity Index; PDI: 0.63 improvement from 0.63 to 0.32) (Fig. 1E). The drug loss from removal of these larger aggregates represented a small (<5%) proportion of Insulin. For fully complexed PLR-Insulin (2.77 μg PLR/μg Insulin), Insulin-GET NCs were formed at 200–450 nm (number distribution) size with some larger aggregates (700–950 nm) present (PDI >0.5) (Fig. 1F). We examined more closely the size distribution of Insulin compared to Insulin-GET NCs. Insulin at physiological pH displayed a wide size distribution with average diameter of 147 nm, (PDI ~0.628), This could be attributed to Insulin's inherent property to form oligomers (dimers & hexamers). However, removal of these aggregates by centrifugation, sizes of 3.75 nm (PDI ~0.32) were achieved (DLS and TEM: Figs. 1E, and DLS: Fig. 1G) with a negative surface potential of -14.1 mV (Zeta: Fig. 1H). For Insulin-GET NCs, the average particle size was 140 nm, (PDI ~0.37) (DLS and TEM: Fig. 1F, and DLS: Fig. 1G), these NCs were highly positively charged with surface potential of +28.16 mV (Zeta: Fig. 1H). This demonstrated PLR was able to bind Insulin through electrostatic interaction, leading to formation of small and stable positively charged NCs. Shift of multiple peaks to single peak towards larger particle size, also confirmed the formation of NCs. These data confirm the size distribution in agreement between DLS measurements and TEM.

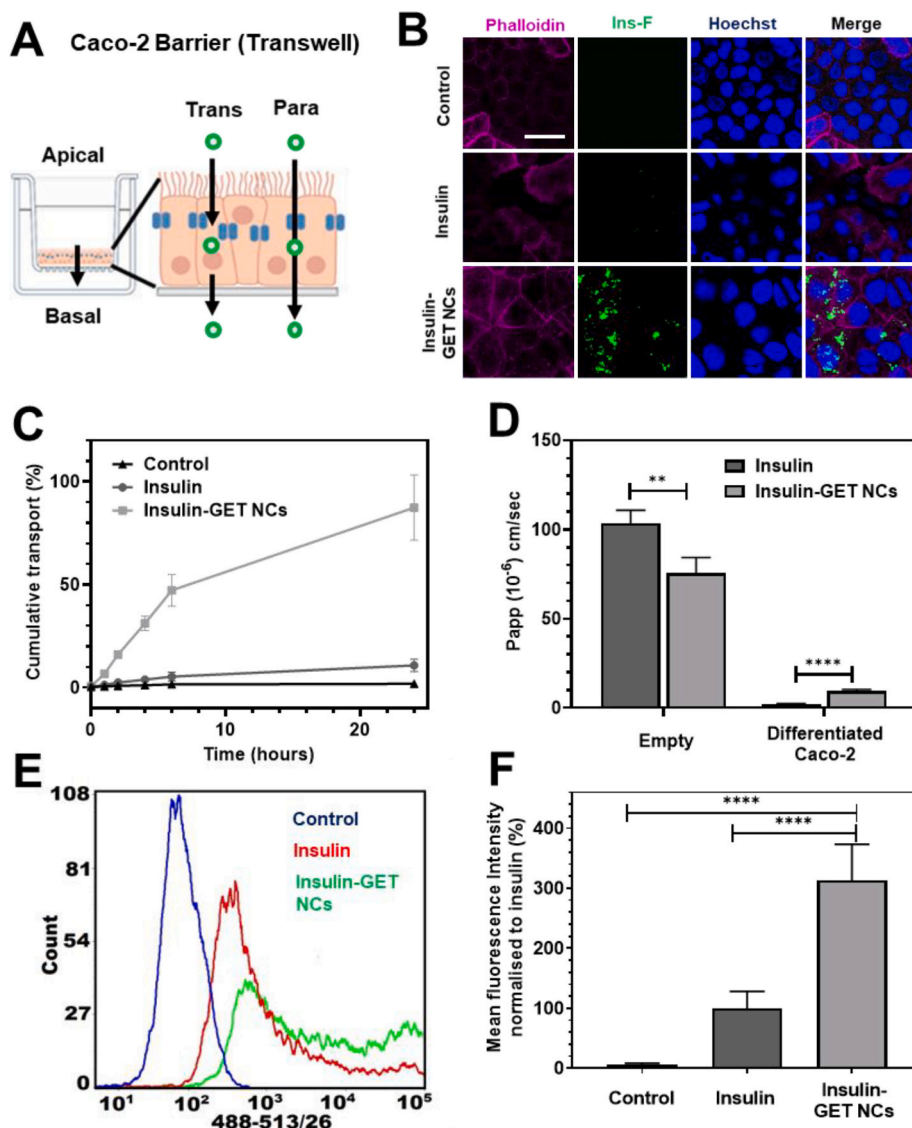


Fig. 2. GET-mediated enhanced Insulin transport across an *in vitro* intestinal model. A. Schematic of the differentiated Caco-2 cell transwell system used for assessing Apical to Basal transport of Insulin. Transcellular (through cells) and paracellular (between cells) routes are depicted. B. Confocal microscopy of Phalloidin (actin cytoskeleton) counter stained Ins-F delivered as Insulin-GET NCs (Blue is Hoechst counterstain) Bar is 10 μm. C. Cumulative transport of Insulin compared to Insulin-GET NCs (using Ins-F) across the Caco-2 barrier. GET enhances Insulin transcytosis efficiency by >22-fold, leading to more apical-basal and basal-apical transport. D. Papp values (10⁻⁶ cm/s) at 6 h post-delivery showing increased permeation for Ins-GET NCs through the Caco-2 barrier compared to empty transwells. E. Flow cytometric histogram analysis demonstrating GET significantly enhances cellular internalization of Insulin. F. Cellular uptake and internalization quantification for Ins-F and Ins-F-GET NCs at 6 h by flow cytometry. The values represent mean ± S.D., n = 6, * = p-value <0.05, ** = p-value <0.005, *** = p-value ≤0.0005, **** = p-value <0.0001, and ns = not significant. 2-Way ANOVA with Tukey's test. (For interpretation of the references to colour in this figure legend, the reader is referred to the web version of this article.)

3.4. Insulin-GET NCs have enhanced permeability through intestinal cell models *in vitro*

Caco-2 cells are human colorectal carcinoma cells that can be differentiated into an intestinal layer with tight-junctions and forms a barrier for intestinal absorption studies [44,45]. The intestinal absorption (uptake into cells) and transport (across the barrier) properties of

Insulin and Insulin-GET NCs was compared *in vitro* within the transwell-differentiated Caco-2 cell monolayer model. These differences allow for assessment of trans- and paracellular transport (Fig. 2A). We used fluorescently-labelled Insulin (Ins-F) which was detectable by fluorometry, microscopy and by flow cytometry. Insulin was poorly transported into cells (Fig. 2B). Confocal microscopy using labelled Insulin and cytoskeletal staining (Alexa-Fluor 647 Phalloidin) clearly showed the

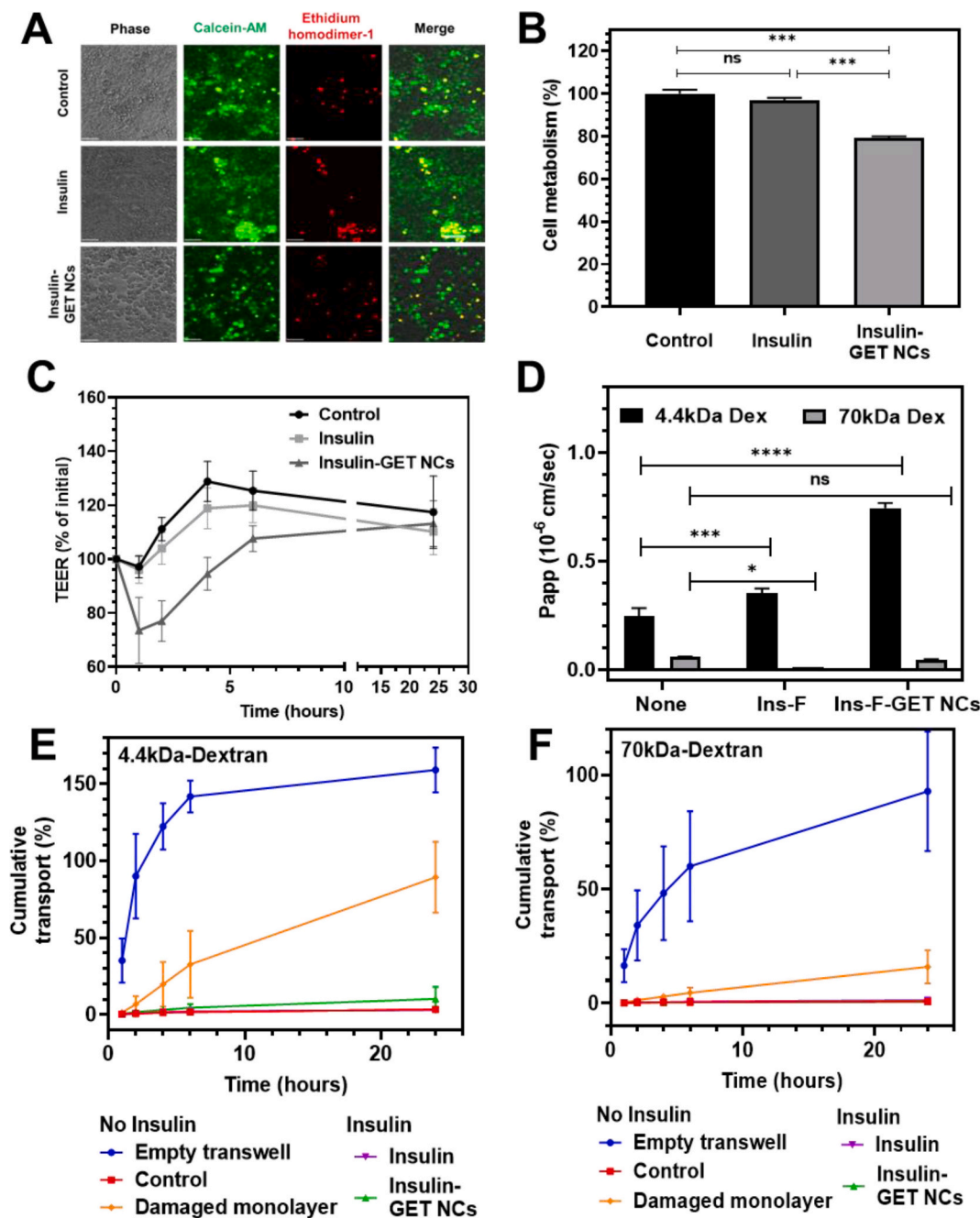


Fig. 3. Intestinal Barrier model integrity is retained during GET-mediated enhanced delivery of Insulin. **A.** Live/Dead staining of Caco-2 monolayers with Insulin or Insulin-GET NC delivery (24 h exposure). This demonstrates that there is no enhanced cell death in GET-treated samples (at the 10 μ M PLR dose: 10 μ g Insulin tested). Bar is 50 μ m. **B.** Metabolic assays (PrestoBlue) of Caco-2 monolayer treated as for **A.** showing that there is a minor reduction in metabolic activity with Insulin-GET NC administration. **C.** TEER values depicting monolayer integrity is maintained throughout administration. Data shows a transient reduction in TEER values with GET-mediated delivery which recovers the majority by 6 h and fully by 24 h. **E-F.** Permeability assay using different molecular weights (MW) of labelled (TRITC) Dextran (Dex). Data demonstrates that monolayer integrity is maintained during delivery. **E.** Cumulative transport for 4.4kDa Dextran across Caco-2 monolayers under different conditions. Controls consisted of transport across untreated cells (no transfection, just delivery of dextran) as a positive control empty transwells with no cells were used to assess transport in absence of any barrier. **F.** Cumulative transport for 70kDa Dextran under the same conditions. All values are presented as mean \pm S-D, $n = 3$, * = p -value < 0.05, ** = p -value < 0.005, *** = p -value \leq 0.0005, **** = p -value < 0.0001, and ns = not significant. Mixed effect analysis and One-way ANOVA with Tukey's test.

difference in relative uptake of Insulin with and without GET, where GET greatly enhanced the cellular uptake and internalization of Insulin. Transverse, cross-sections, show significantly greater cellular permeation and accumulation, where Insulin-GET NCs were seen widely distributed throughout the cell monolayers with localization in different cellular regions, with the predominant signal in perinuclear vesicles. Insulin transport across the intestinal model (apical to basal diffusion) (Fig. 2C), was significantly enhanced with the GET-peptide system. The transcytosis efficiency of the optimal Insulin-GET NC formulation was ~22-fold greater than the Insulin alone (Fig. 2C). We confirmed that not only the Ins-F variant of Insulin was enhanced by GET, and repeated delivery experiments to Caco-2 barriers in growth media (GM) and serum-free media (SFM) but also with quenched Ins-F* (Fig. S2), and unlabelled recombinant Insulin (uptake and transcytosis quantified by ELISA) and TRITC labelled Insulin (Ins-T, by fluorometry and flow cytometry) (Fig. S3). Importantly fluorescence-based experiments correlate well with unlabelled Insulin directly detected by ELISA.

The P_{app} values of Insulin-GET NCs (9.35×10^{-6} cm/s) were significantly superior to Insulin (1.98×10^{-6} cm/s) across Caco-2 monolayers in shorter (6 h) incubations (Fig. 2D). After prolonged exposures (24 h), P_{app} values were slightly reduced (5.14×10^{-6} versus 1.05×10^{-6} cm/s, respectively), however this is likely to be reflective of the reduction in concentration in the apical chamber due to enhanced cell uptake and transport by GET complexation. GET-mediated delivery therefore increases the transepithelial permeation of Insulin by ~6-fold compared to Insulin alone. Assessing cell uptake by flow cytometry demonstrated that Insulin was up taken at low levels, however Insulin-GET NCs has enhanced up take (>3.2-fold more) (Fig. 2E, F).

3.5. Insulin-GET NCs is not cytotoxic and does not disrupt the intestinal barrier integrity or electrical resistance

It was important to assess any effect on cell viability or metabolism by incubation with Insulin-GET NCs. We therefore assessed viability with LIVE/DEAD assays and metabolic effect of delivery using resazurin-based PrestoBlue assays (Fig. 3). Insulin alone showed negligible cytotoxicity (Fig. 3A) or metabolic effect (Fig. 3B) compared to controls. In contrast, although only the highest doses of Insulin-GET NCs, generated an increase in dead cells (>50 μ M), there was a statistically significant decrease in metabolism (Fig. 3B and not shown). Despite this reduced metabolism this was a transient effect below 20 μ M GET, with full recovery after longer-term exposures (~98.7% of untreated 24 h post-removal), or if the formulation was removed. This demonstration confirms that the primary mechanism of enhanced permeability is not by simple loss of barrier viability and that the system is cytocompatible.

If exposure to Insulin-GET NCs damaged or generated leaky barrier function then we would falsely conclude Insulin transcytosis. It was vital to confirm that simple removal of barrier integrity was not responsible for enhanced Insulin transport. Transepithelial electrical resistance (TEER) measurements were employed to confirm differentiation and barrier function initially before delivery experiments ($\sim 960 \pm 50 \Omega/\text{cm}^2$). This reading confirms membrane tight-junction integrity and the validity of the model. We employed TEER to assess any compromised barrier function during and after Insulin-GET NC delivery. In comparison with control (untreated cell monolayers), a statistical insignificant decrease was observed in TEER values upon incubation with either free Insulin or Insulin-GET NCs (Fig. 3C). TEER values immediately fell to $90 \pm 12\%$ and $70 \pm 20\%$ of initial values within 30 min of exposure, for both Insulin and Insulin-GET NCs, respectively. Further monitoring of TEER demonstrated that the drop was transient, as values recovered to baseline values for controls even if the formulation was not removed (Fig. 3C). This indicated that the change in TEER may be artefactual or generated transiently by Insulin delivery or through the mechanism of enhanced uptake by GET.

To adequately determine the effect of GET-peptide on monolayer integrity and cellular uptake mechanism (paracellular or transcellular

pathway), transport of hydrophilic tracers *i.e.*, low and high molecular weight (MW) dextran (4.4 kDa and 70 kDa), fluorescently-labelled (TRITC), was examined across monolayers during Insulin-GET NC exposure. We initially compared empty transwells to those with differentiated Caco-2 monolayers to confirm the baseline for fully porous *versus* completely intact barriers within the model (Fig. S4). The cumulative transport (CT) of Dextran was remarkably reduced compared to controls *i.e.*, 3.4% and 0.65% for 4.4 kDa- and 70 kDa-Dex, respectively, with an intact intestinal cell barrier. P_{app} values for 4.4 kDa-Dex (1.27×10^{-6} cm/s) was ~19-fold greater than for 70 kDa-Dex (0.066×10^{-6} cm/s) which was expected due to size inhibition (Fig. 3D). Apical application of Insulin-GET NCs (10 μ M PLR) increased the transport/permeability rate of 4.4 kDa- and 70 kDa-Dextran by 3-fold (10.2%) and 1.6-fold (1.5%), respectively (Fig. 3E and F). With the optimal GET concentration (10 μ M), generating P_{app} values for 4.4 kDa-Dextran (0.743×10^{-6} cm/s) was ~16.5-fold greater than for 70 kDa-Dextran (0.045×10^{-6} cm/s). Chemically damaging monolayers (pre-treatment with 5 N NaOH) resulted in dramatic increase in CT (4.4 kDa- and 70 kDa-Dextran by 90% and 16%, respectively) showing that the effect of GET was minimal in comparison to actively destroying the barrier.

3.6. Insulin-GET NCs penetrate intestinal barriers through transcytosis

To determine if barrier penetration was para- or transcellular, we examined the cellular absorption and internalization of Insulin by microscopy and flow cytometry of disaggregated Caco-2 cells recovered from the barrier during and after exposure. Conventional flow cytometry (Fig. 2E, F) and microscopy (Fig. 2B), agreed with ImageStream analyses (imaging flow cytometry, Fig. S5) which confirmed a significant increase in cell association and internalization at time-points early (1 h) and late in Insulin-GET NC exposure.

As cell association (either on the cell membrane or internal to cells) was significantly promoted as Insulin-GET NCs compared to Insulin alone, we examined if Insulin was exported from delivered cells after exposure had ended. This data showed that over-time cells that had been loaded, which we term 'depotized' (Fig. 4A), with Insulin-GET NCs released their Insulin (fluorometry; Fig. 4B, C) and that this loss resulted in lower internalized Insulin (flow cytometry, Fig. 4D, E). We wanted to assess the relationship between uptake and release of Insulin and GET concentration. Steady state levels of internalized Insulin was dependent on GET peptide concentration during exposure (Fig. 4D) showing the direct and proportional effect of GET on uptake. After uptake, release of the uptaken Insulin was proportional to that initially loaded into cells by GET (Fig. 4E), except for higher concentrations of GET (>20 μ M) which affected viability. Therefore, we confirmed that Insulin indeed was being uptaken and exocytosed by GET complexation primarily via intracellular trafficking.

3.7. GET and insulin-GET NC can increase non-specific uptake and release which is bidirectional

GET does not damage barrier integrity but does minimally improve transport of Dextran. Therefore, the system may either induce an ineffective paracellular pathway or promote non-specific uptake/secretion of molecules exposed to cells. We have previously shown that GET enhances endocytosis significantly promoting low level uptake of non-complexing molecules (Bovine serum albumin, BSA) or efficient uptake of nanoparticles coated with Dextran [9,14]. Enhanced cellular uptake was observed for both Dextran sizes (Fig. S4) to a similar magnitude as that seen for enhanced permeability (data not shown). We therefore hypothesize that paracellular pathways by GET are likely to be minimal and transcytosis, even of non-complexed molecules, at a low level is possible with high dosages of GET.

The apical-to-basal transport was key to oral Insulin delivery demonstration; however, we had not determined if the uptake/export transcytosis mechanism in this system was directional (Fig. 5A). We

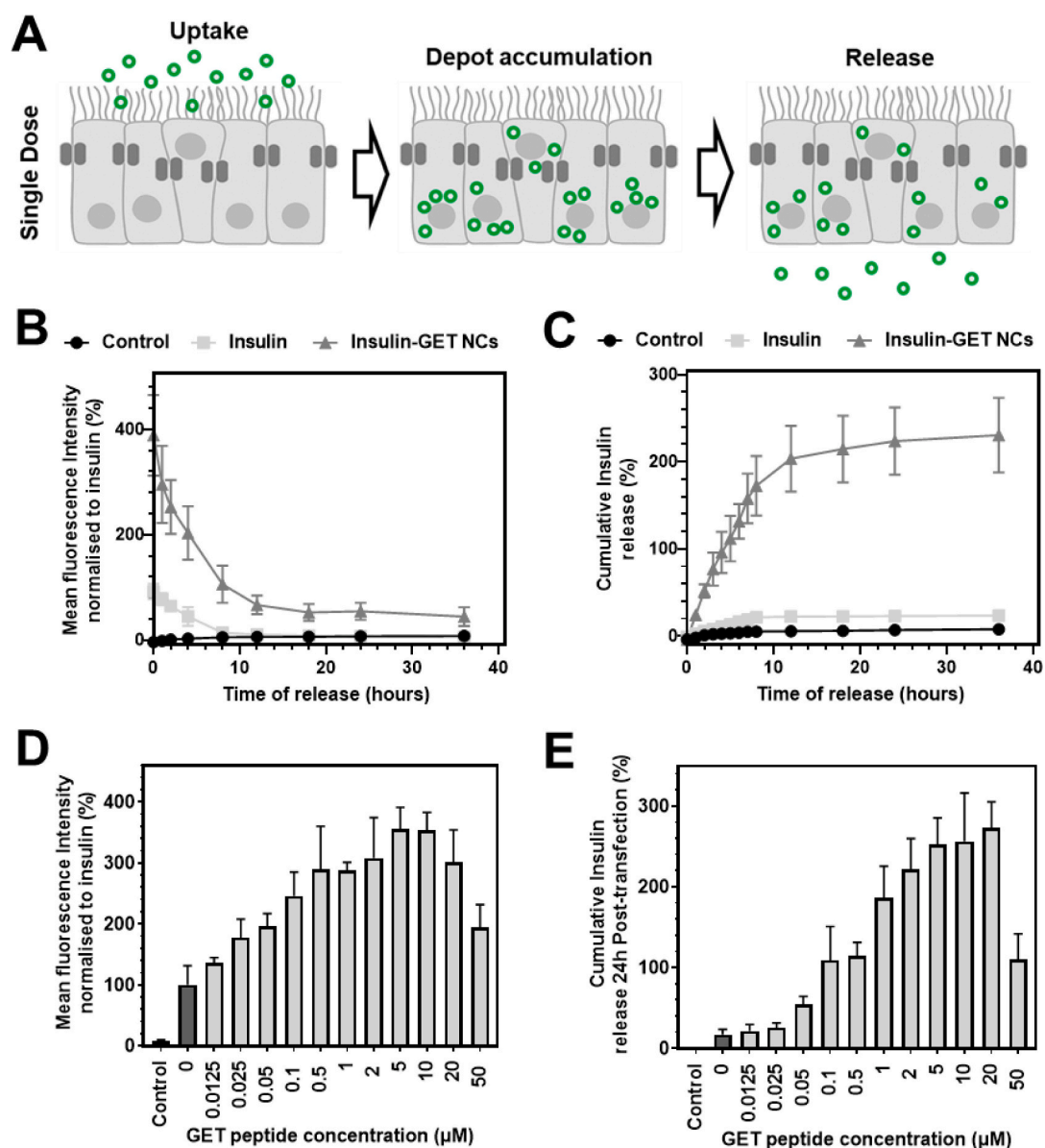


Fig. 4. Insulin Depotization of Caco-2 cells and post-release kinetics. A. Schematic of the depotization of Caco-2 cell monolayers with Insulin-GET NC delivery generating large intracellular stores of Insulin that are progressively released post-delivery B-C. Caco-2 monolayers were incubated with Insulin-GET NCs (10 μg Insulin, 10 μM PLR) and B. cell fluorescence (mean fluorescence intensity normalized to Insulin only at 0 h timepoint) determined by flow cytometry, and C. Cumulative Insulin release (normalized to that release from Insulin only during transfection for 24 h) determined by fluorometry. This demonstrates that after delivery Insulin is progressively released from the monolayer plateauing at ~ 12 h with a reciprocal loss of internalized Insulin. D. Caco-2 internalized Insulin levels using different dosages of PLR peptide (0.0125–50 μM with 20 $\mu\text{g}/\text{ml}$ Ins-F) and E. post-transfection release of Insulin in the subsequent 24 h with different PLR dosages. This demonstrates that higher PLR (up to ~ 5 μM dose) is required for the maximal release of Insulin, however uptake levels were generally enhanced by lower levels of PLR (0.5 μM dosages). All values are presented as mean \pm S-D, $n = 5$, * = p -value < 0.05 , ** = p -value < 0.005 , *** = p -value < 0.0005 , **** = p -value < 0.0001 , and ns = not significant. Mixed effect analysis with OrdinaryOne-way and Two-way ANOVA with Tukey's test.

conducted experiments in the basal to apical direction (Fig. 5B) and pulse-chase experiments were Insulin-GET NCs were delivered and the release from cells back into the apical or through the barrier into the basal chambers were measured. Fluorometry showed that cell-associated Insulin delivered by GET complexation could be exported back apically or transcytose basally (Fig. 5C). To extend these analyses we assessed if initial uptake itself was directional, examining apical-to-basal, compared to basal-to-apical transport (Fig. 5D). Indeed, we could demonstrate evidence for both directions of travel and that although uptake and transport was preferential in the apical-to-basal orientation, that GET seemed to generically promote uptake and release of Insulin from cells.

3.8. Insulin-GET NC stability activity is retained intracellularly and post-transcytosis

To assess the stability of Insulin-GET NCs directly in cells we repeated cell uptake and transcytosis assays but directly compared the delivery of non-quenchable (Ins-F) to quenchable (Ins-F*) variants. It was clear that using quenchable Ins-F*, the Insulin delivery was dramatically underestimated if comparing both variants (Ins-F* having 5-fold lower fluorescent levels that Ins-F delivered in SFM) (Fig. 5). We used Caco-2 cell lysates to investigate the differences in fluorescence post-delivery and therefore the stability of internalized NCs after translocation, compare to those exported (Fig. 5E). Cell samples with delivered Insulin-GET NCs were assessed by fluorometry with and

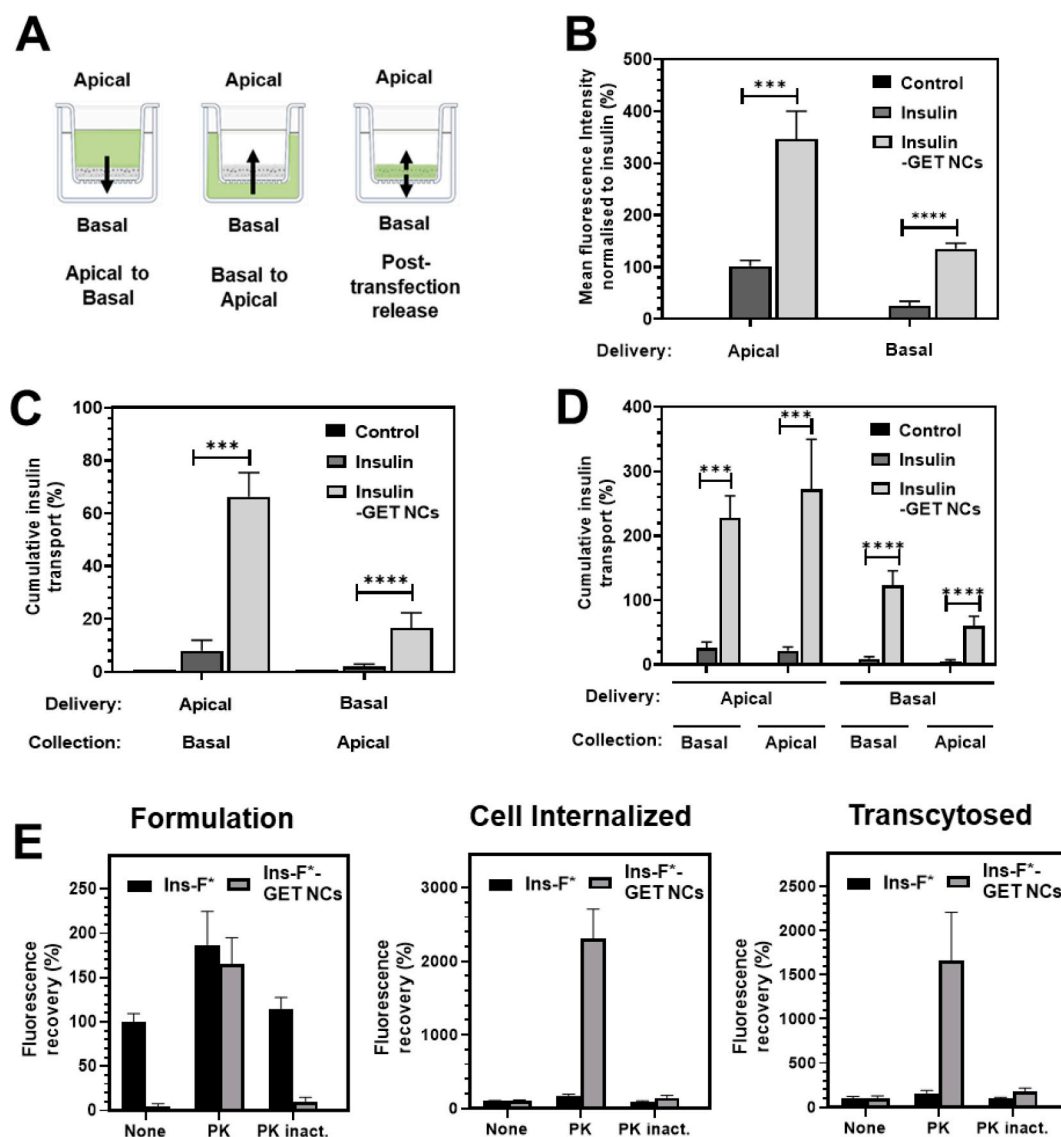


Fig. 5. Non-directional uptake and release of Insulin by GET-mediated enhanced delivery. A. Schematic of the Caco-2 transwell system used for conventional Apical to Basal testing, as well as Basal to Apical, and Apical or Basal Insulin release from pre-delivered Caco-2 barriers. B. Caco-2 monolayers were incubated with NCs in SFM and the internalization of Insulin quantified by flow cytometry either Apically or Basally (data normalized to Apical level generated by Insulin alone). This demonstrates that GET can enhance delivery of Insulin from Apical or Basal administration. C. Cumulative Insulin transport across the Caco-2 barrier (Apical to basal or Basal to Apical) in the same conditions as B. This demonstrates that transport is enhanced with GET across the barrier irrelevant of Apical or Basal administration. D. Pre-delivered Caco-2 monolayers were assessed for release of Insulin in the context of side of administration for both the same or opposite side of release. This demonstrates that irrelevant of the side of administration that Insulin is transported to the same or opposing side more efficiently with GET. E. Dequenching the fluorescence of cell internalized and transcytosed Insulin-GET NCs by proteolysis. Recovery of fluorescence quenched Ins-F* induced upon complexation with GET peptide by incubation of freshly generated formulations (left), Caco-2 monolayers delivered for 24 h (middle) or transcytosed basal media after 24 h delivery digested with Proteinase K (PK) (0.2 $\mu\text{g}/\mu\text{l}$) at 37 °C. Controls were also completed with heat-inactivated PK showing no dequenching activity. All values are presented as mean \pm S-D, n = 5, * = p-value <0.05, ** = p-value <0.005, *** = p-value <0.0005, **** = p-value <0.0001, and ns = not significant. Mixed effect analysis with Ordinary One-way and Two-way ANOVA with Tukey's test.

without PK-treatment (at room-temperature) for both Insulin variants. Fluorescence intensity was increased progressively time-dependently (data not shown) at a similar rate to non-delivered control Insulin-GET NCs generated from quenchable Ins-F* with minimal increases from Ins-F. Importantly this was not the case for free-Insulin delivery from either Ins-F or Ins-F* which both increased only marginally when digested. Additionally, exposing samples to increased temperature (56 °C for optimal PK activity) completed proteolysis to demonstrate the maximum dequenching of Fluorescein fluorescence. It was clear that most of the Insulin inside of cells delivered by GET was still complexed.

Likewise, media samples containing transcytosed NCs were collected from basolateral chamber of transwell and PK-digested for both variants

(Fig. 5E). The results indicated that NCs were stable and still intact after transcytosis, where quenched fluorescence of Ins-F* samples recovered over time. We therefore conclude that GET can form stable complexes with Insulin via electrostatic interactions, such that GET-peptide remained bound to Insulin during transcytosis.

3.9. Modulation of cellular endocytotic uptake, recycling and export from cells determines Insulin transcytosis

To understand the mechanism of transcytosis of Insulin-GET NCs more closely we investigated intracellular uptake, trafficking and endosomal recycling using different endocytosis and secretion

modulators (Fig. 6). Although transport of Insulin was hypothesized to be largely impacted by GET peptide properties, we reasoned that if free intracellular Insulin trafficking was mediated by endogenous regulatory processes, then we would have a more complete understanding of the

transcytosis mechanism and how to exploit it. GET is known to mediate uptake through heparan sulfate-membrane binding to stimulate macropinocytosis and uptake into vesicles. Vesicular-sequestered cargos delivered with GET appear to have longer half-lives than would be

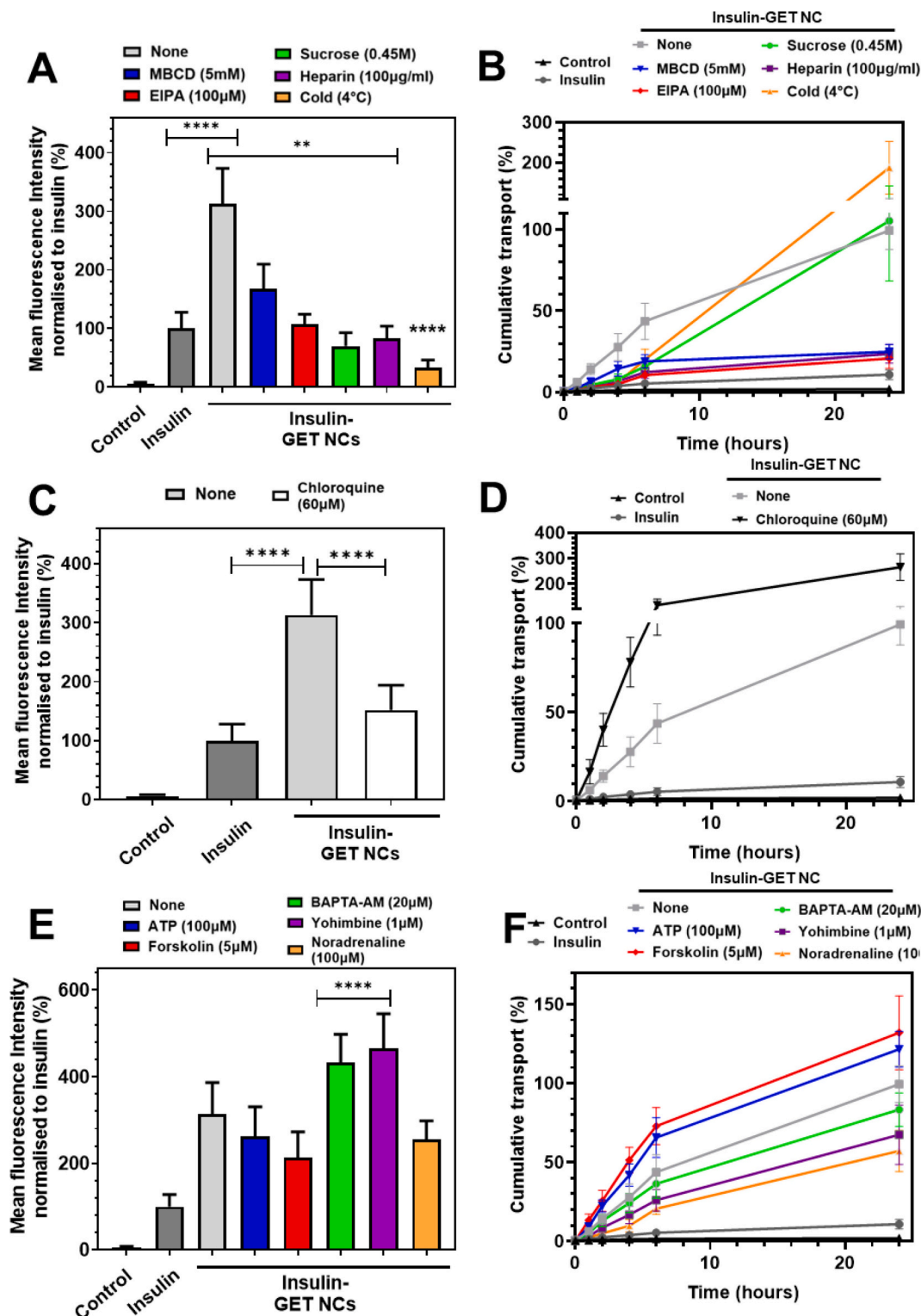


Fig. 6. Endocytosis, endosomal escape and export mechanisms are required for efficient uptake and transcytosis of Insulin-GET NCs. Caco-2 monolayers were incubated with Insulin or Insulin-GET NCs in presence of A & B. endocytosis inhibitors, C & D. chloroquine for endosomal escape, or E & F. intracellular trafficking inhibitors, and cell uptake of Ins-F determined by flow cytometry (24 h exposure) (A, C, E). Cumulative release of Insulin and Insulin-GET NCs in the presence of inhibitors determined by fluorometry (B, D, F). All values are presented as mean \pm S.D., $n = 5$, * = p -value < 0.05 , ** = p -value < 0.005 , *** = p -value < 0.0005 , **** = p -value < 0.0001 , and ns = not significant. Two-way ANOVA with Tukey's test.

expected. However, some cargo can be shown to escape vesicles to be relocalized and functional [10]. We investigated the uptake, release and secretion of Insulin in our barrier model using small molecules to determine the mechanisms involved in Insulin-GET NC transcytosis. We employed high concentration Heparin (100 µg/ml) to detach external Insulin-GET NCs to distinguish between cell membrane localized and internalized Insulin [9] (Fig. 6A). It was clear that high Heparin concentration could both disrupt Insulin:GET interaction, and uptake and therefore release of Insulin (Fig. 6B), respectively. Low temperature (4 °C) rigidifies the cell membrane and slows passive and active uptake [46]. This inhibition was confirmed for uptake (Fig. 6A) and for transcytosis except for prolonged incubations (>6 h) where the barrier was disrupted (Fig. 6B). 5-N-ethyl-isopropyl amiloride (EIPA), an inhibitor of Na⁺/H⁺ exchange required for macropinocytosis [47], caused decreased internal Insulin levels and transcytosis, but did not affect cell association (Fig. 6A, B), thus confirming that cellular uptake of these NCs ensues via energy-dependent pathways as previous studies [48]. Hypertonic conditions (employing sucrose) that hinder clathrin lattice formation [49], decreased both association and uptake (Fig. 6A, B) but damaged barrier integrity with long-term incubations (>6 h). Methyl-B-cyclodextrin (MBCD) that represses caveolae-mediated endocytosis through complexation of cholesterol [50] did not affect cell association but inhibited uptake and overall transcytosis. As endosomal uptake appeared key to Insulin-GET NC transport, we assessed if endosomal escape-enhancing molecule, Chloroquine (Fig. 6C, D), could also affect internal and released levels of Insulin [51]. Chloroquine treatment yielded lower levels of internalized Insulin (Fig. 6C) but enhanced levels of transport (Fig. 6D), which we hypothesize was not through an effect in inhibiting uptake. Importantly, this mirrored enhanced cumulative transport across the barrier.

We next looked to assess the mechanisms of intracellular trafficking (Fig. 6E, F). Native secretion of Insulin from pancreatic β-cells is known to be regulated by a variety of intracellular signals generated by glucose, amino acids, and fatty acids, and through neural or hormonal inputs [52]. We tested a panel of small-molecules known to affect intracellular trafficking and secretion of Insulin. BAPTA-AM (BA) (a cytosolic Ca²⁺ chelator) which blockades Insulin secretion by depleting cellular Ca²⁺ [53], showed increased cellular contents and slightly lower levels of overall Insulin secretion. Noradrenaline (NA), a powerful inhibitor of Insulin secretion and endocytosis [48] and Ca²⁺-evoked exocytosis [54,55], had a small but significant effect over Insulin cellular levels, however dramatically reduced Insulin export (Fig. 6E, F). Yohimbine (YB) (an alpha 2-adrenoceptor antagonist) inhibits ATP-sensitive K⁺ channels in β-cells and increases Insulin secretion [56], led to accumulation of Insulin and reduced secretion. Forskolin (adenylate cyclase agonist) that increases cellular levels of cAMP which enhance Insulin secretion [57], inhibited accumulation of intracellular Insulin but enhanced secretion in our model (Fig. 6E, F). This was a similar effect seen to that of addition of high concentrations of ATP, which produced lower levels of uptake with increased secretion. Taken together it's clear that cAMP and Ca²⁺ signaling have some role in regulating Insulin secretion in this artificial cell model. These similarities with trafficking mechanisms in pancreatic β-cells will require further careful elucidation within our model and *in vivo*.

3.10. Insulin-GET NCs offer insulin protection in harsh GI conditions and during transcytosis

Using the quenching assays, we examined the behaviour and stability of Insulin and Insulin-GET NCs in biorelevant media mimicking the gastrointestinal (GI) environment (Fig. S6). Fluorescence of free Ins-F* remained constant in biorelevant medias, FaSSGF and FeSSIF, over time but in presence of Pepsin (Pep) or Pancreatin (Pan) proteolytic enzymes (FaSSGF and FaSSIF, respectively) fluorescence intensity progressively increased over time compared to controls. Additionally, FaSSIF without enzymes also caused a small but significant increase in

fluorescent values for Ins-F* which could be attributed to buffer components. Similarly, Insulin-GET NCs retained low fluorescence intensity in FaSSGF, FaSSIF, and FeSSIF (Fig. S6B). Within FaSSGF+Pep and FaSSIF+Pan progressive fluorescence dequenching was observed time-dependently due to proteolytic action of enzymes. Insulin-GET NCs displayed highest fluorescent values in FaSSIF+Pan indicating that Pan was more active than Pep, disrupting complexes within 10–30 min.

3.11. Insulin biological activity is retained post-transcytosis

As our results indicated that Insulin-GET NCs have enhanced transcytosis, it was important to determine that Insulin retains its biological activity by functional assay. (Fig. 7). For this, we employed iLite Insulin-reporter cells, which transcriptionally respond by increasing transgenic Luciferase expression of an Insulin-responsive gene (Fig. 7A) [58]. Insulin-GET NCs were compared to free-Insulin as a positive control and GET-peptide alone was used as negative control. Insulin alone caused 4-fold reporter induction (Fig. 7B), while increasing GET concentration progressively reduced induction. At the highest Insulin concentrations 5.5iU or 200 µg/ml, the Insulin-responsive reporter was also suppressed, with 0.55iU/ml (20 µg/ml) showing maximum induction. The reduction in functional activity of Insulin with increasing GET complexation was concentration-independent beyond 12.5 nM (Fig. 7C), as this produced similar reduction to the highest concentration (50 µM). Overall, Insulin-response was reduced ~50% (2-fold induction) with GET complexation; however, Insulin did retain significant biological activity as Insulin-GET NCs.

Next, we analysed the ability of Insulin-GET NCs to retain functional activity post-transcytosis with the transwell releasate used to activate iLite cells (compared with the freshly prepared NCs and Insulin as positive controls). We employed non-quenchable, fluorescently labelled Insulin (Ins-F) as this allowed the concentration of Insulin to be quantified in basolateral chamber and the Insulin concentration normalized by dilution (20 µg/ml) so the same stimulation was possible. We found that post-transcytosis, both free and Insulin-GET NCs were only marginally lower in biological activity to controls (Fig. 7D). When comparing collected Insulin and Insulin-GET NCs, there was slightly increased induction with Insulin-GET NCs compared to free-Insulin. As Insulin concentration was estimated and normalized using fluorometry, it may be possible that free-Insulin was more degraded than Insulin in Insulin-GET NCs and therefore resulted in lower biological responses when tested. There was insignificant difference in the induction capability of freshly prepared and post-transcytosis Insulin-GET NC released samples, thereby reflecting no loss of functional activity after translocation through Caco-2 monolayers. Similarly, decreased induction of iLite cells by Insulin-GET NCs compared to Insulin agreed with the previous results, where Insulin complexation by GET lowered its functional capability. We therefore conclude that translocated Insulin and Insulin-GET NCs are sufficiently stable and efficiently retained functional activity, providing evidence that Insulin-GET NCs are likely to be biologically and pharmacologically active.

3.12. Oral delivery of Insulin-GET NCs at defined GET dosages can mediate sustained reduction in blood glucose

The ultimate demonstration of the Insulin-GET NC is to examine their pharmacological activity *in vivo*. We exploited the Streptozotocin (STZ)-induced diabetic mouse model, which represents a well-established animal model of type-1 diabetes (Fig. 8). These animals exhibit very high blood glucose levels (BGLs) and respond well to injected subcutaneous or intraperitoneal Insulin (2iU/kg) producing a rapid and sustained reduction in hyperglycemia (Fig. 8A). This was important as in normoglycemic mice there is a narrow window for modulating BGL without arousing counter-regulatory responses, and lacking endogenous Insulin influence. For clinical application of oral Insulin most relevant administration would be administer before meals

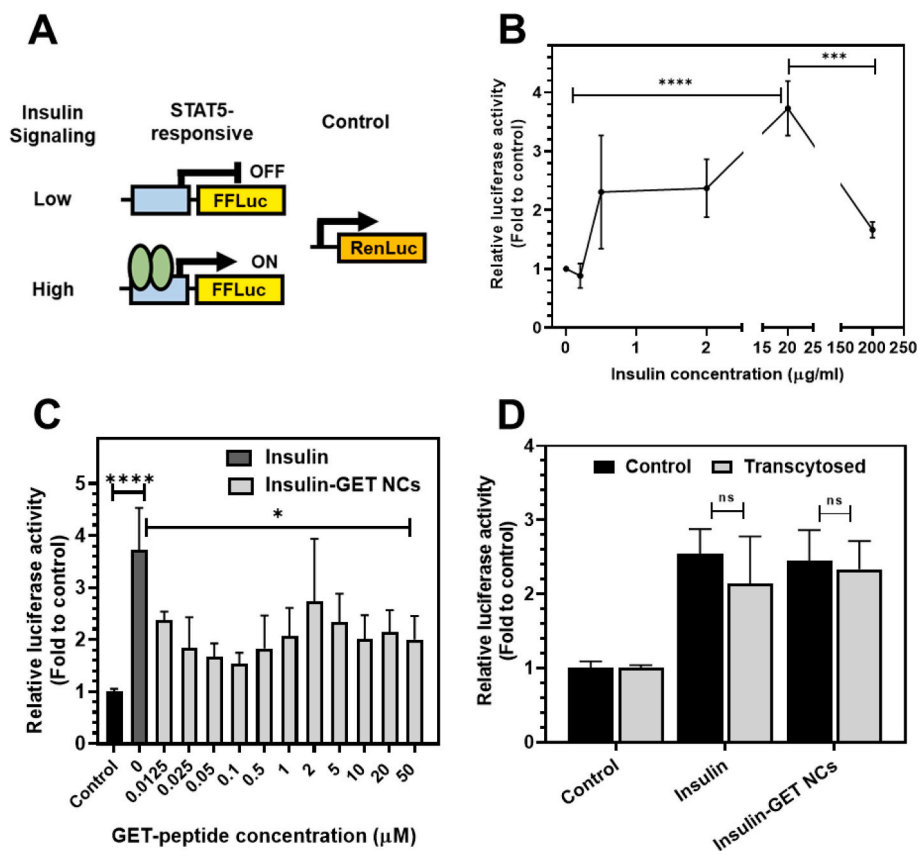


Fig. 7. Insulin retains biological activity as a GET NC and post-transcytosis. A. Schematic of the Insulin functional assay employed with Insulin-responsive iLite cells. iLite cells contain a STAT5-responsive FFLuc reporter which is activated by Insulin signaling following exposure to Insulin. This is a relative assay using a nonresponsive RenLuc reporter as a control for assay loading. B. Titration of Insulin dose in iLite cell assay with 20 µg/ml being optimal response. C. Insulin alone (20 µg/ml optimized concentration) enhances STAT5-responsive reporter expression ~4-fold in iLite cells. Addition of GET peptide (PLR) even at low levels (0.0125 µM) reduces the magnitude of activation but still allows Insulin to enhance STAT5-response reporter expression (~2-fold). This is the case even for high dosages of PLR (up to 50 µM). D. Functional assays were performed with freshly prepared (control) or transcytosed Insulin and Insulin-GET NCs (10 µM PLR). Insulin concentration was normalized with ELISA to 20 µg/ml for stimulation. This demonstrates there was minimal difference between overnight transcytosed Insulin compared to control formulations in inducing iLite STAT5-reporter gene expression. All values are presented as mean ± S.D., n = 3, * = p-value <0.05, ** = p-value <0.005, *** = p-value <0.0005, **** = p-value <0.0001, and ns = not significant. One-way ANOVA with Tukey's test.

or after short periods of fasting, therefore our initial studies were using animals in a fasted state.

Initially we confirmed that this model does not respond to even the highest dosages of free-Insulin given orally by gavage (500iU/kg), namely 250-times higher than the injected dose. Using this dose, we compared low (0.1 mM), medium (1 mM) and high (10 mM) dosages of PLR in Insulin-GET NCs and assessed reduction in BGL (Table S2 and Table S3). The lowest (0.1 mM) complexation of PLR generated the greatest response in BGL with hyperglycemic levels (20 mmol/l glucose) being over-reduced to hypoglycemia with animals requiring glucose syrup (Fig. 8B). This effect of Insulin-GET NCs was prolonged (>4 h) and fast-acting (90% reduction within 1 h). A medium PLR dose (1 mM) evoked a smaller decrease in BGL (30% reduction within 1 h) and the highest PLR dose (10 mM) had no effect on BGL. As 500iU/kg is a very high Insulin dose, we moved to use a lower Insulin dose that has been used in other oral Insulin studies (100iU/kg). We were able to demonstrate similar trends with lower dosages being more effective at lowering BGL, assessing area under the curve (AUC) (Fig. 8C). We determined tAUC for the first 4 h post-gavage which showed over >70% reduction in BGL (Blood glucose mmol/l/min). When repeating experiments with lower dosages (down to 20iU/kg) we were able to demonstrate a lowering of BGL if the optimal PLR concentration was employed.

3.13. Insulin-GET NCs have reduced pharmacological activity than free Insulin with intraperitoneal delivery

We have previously shown that Insulin has a reduced biological activity in cell-based *in vitro* functional assays when complexed with GET at high concentrations. We tested the ability of intraperitoneally dosed Insulin complexed to GET compared to high bioavailability free Insulin to reduce BGL in diabetic mice (Fig. 8A). We were able to show that high concentrations of GET (Insulin:GET, 1:5 ratio) indeed did inhibit biological function, this reflective of the formulations most potent in oral

delivery. This confirms that although GET can indeed promote Insulin delivery that the Insulin delivered that remains complexed to GET has reduced biological function.

3.14. Oral dosing of Insulin-GET NCs can correct high blood glucose and improve physiology of diabetic animals

To confirm that orally dosed Insulin-GET NCs can control BGL over a longer period in diabetic mice (Fig. 9), we conducted non-fasting experiments where diabetic mice (with *ad libitum* food and water) were dosed orally with Insulin-GET NCs both in the morning (AM) and afternoon/evening (PM), measuring BGL over a 4-day period (Fig. 9A). These animals exhibited very high BGL unfasted (~40 mmol/l and ~35 mmol/l glucose, for AM and PM, respectively). After the initial dosing (day 0, PM) we could observe a significant lowered BGL (~31 mmol/l) after 17 h, the following morning (day1, AM), repeating oral delivery for AM and PM dosages demonstrated that an AM dose could control BGL at PM measurement (~25 mmol/l) (Fig. 9B) and *vice versa* for at least 4 days (Fig. 9C). Free Insulin alone had no effect and both low and medium dosages of PLR showed similar trends. Both groups with Insulin-GET NC delivery showed lower intake of water (Fig. 9D) and food (Fig. 9E), as well as pronounced increases in bodyweight (Fig. 9F), which were not seen in untreated or Insulin only groups.

4. Discussion

4.1. CPPs as translatable Insulin delivery vectors

Emergence of CPPs as powerful trans-epithelial delivery vectors has the promise of revolutionizing therapeutics, however their use still lacks the efficiency to make viable products for delivery problems such as the oral delivery of Insulin [59]. Simplistic CPPs have been shown capable of penetrating biological membranes at low micromolar concentrations,

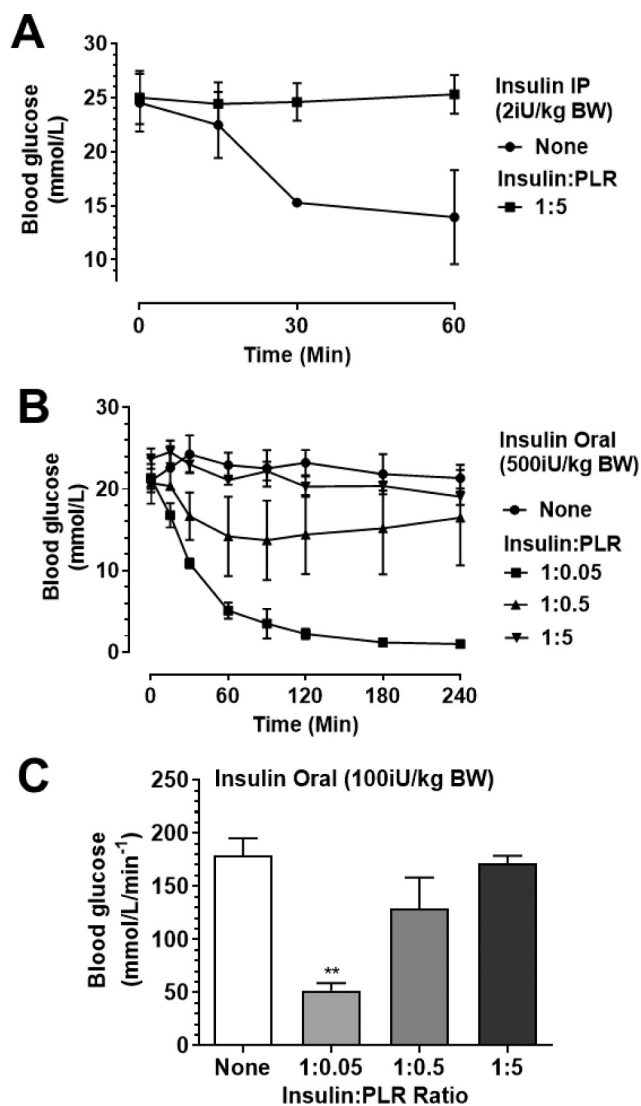


Fig. 8. Insulin-GET NCs have inhibited Insulin activity *via* intraperitoneal injection but have enhanced oral delivery at optimal ratios. A. STZ diabetic mice administered 2iU/kg human insulin alone or in combination with GET at a ratio of 1:5 resulted in no reduction in blood glucose in the Insulin/GET group whereas insulin alone *via* IP injection lowered blood glucose as expected. Furthermore, B. Oral insulin delivery mechanisms were then tested using human insulin alone, or in combination with various GET conjugations. Results indicate oral insulin alone and GET combo at ratio of 1:5 had no effect on blood glucose, whereas insulin/GET ratios of 1:0.5 had shown a positive trend in initial reductions, and finally the GET ratio 1:0.05 resulted in normoglycemic values by 240 min, no hypoglycaemic signs were evident post investigation. C. Blood glucose values expressed as AUC for each treatment group. All values are presented as mean \pm SEM, n = 3, ** = p-value <0.005 *via* Two-way ANOVA.

through adsorption to cell-surface GAGs and subsequently internalized by endocytic pathways [40,60]. Poly-arginine (octa-arginine, 8R) has been effectively employed as promoter of intracellular drug delivery orally, nasally and even to deliver drugs across blood brain barrier into the brain, however such demonstrations have not yielded the transformative approaches promised over a decade ago. We developed the GET system to overcome the need for excesses to drive uptake. Here, the GET system was able to significantly improve the intracellular permeation/uptake, delivery, and transcytosis of insulin >22-fold compared to free Insulin (Fig. 2C). This is a very simplistic complexation formulation, mixing a synthesized peptide with Insulin. Here, the level of uptake outperforms the systems of other studies, and our data show that the

recycling mechanisms for Insulin-GET NCs are unique, with observations suggesting that cells function as depots of exogenous Insulin for sustained delivery. Our approach of simple complexation by mixing two electrostatically attracted components is translatable. Insulin-Tat (CPP), as a covalent conjugate, has been shown to enhance Insulin permeability by ~6-fold across Caco-2 monolayers but requires chemical conjugation [61]. Similarly, co-administration of Insulin with CPPs 8R, Penetratin, RRL helix, and pVEC peptides showed significant improvement of insulin ileal absorption in rats [62]. However, none have achieved the levels of improvement we demonstrate, nor the metabolic regulation we observed *in vivo* in diabetic animals. Importantly Insulin could be exploited as a model peptide for oral administration using GET, meaning that other peptide therapeutics (e.g., Incretin mimetics, GLP1) could be developed for oral delivery.

4.2. Insulin-GET does not compromise viability or integrity of intestinal barriers

As GET does not compromise the integrity or viability of our intestinal models. A slow decline in TEER (5–25% over a 4 h period, initially 25% which was reduced to 5% in 4 h period) was observed on incubating Insulin-GET NCs similarly to other studies, but TEER values stayed unaffected upon incubation with Insulin alone [63]. These values recovered upon exhaustion of the formulation or removal of the formulation from incubation. For non-specific permeability, it has previously been shown that apical application of CPPs (PIP peptides 640 and 250) cause transient, reversible and non-toxic reduction of Caco-2 monolayer TEER values, resulting in opening of selective paracellular routes [64]. We have shown that lower MW dextran transport increased more than higher MW variants during the exposure of cells to GET. This agrees with previous studies where effectiveness of enhancement was reduced with increasing MW of Dextran [65]. We did not perform cytotoxicity studies *in vivo*; however, we saw no evidence of negative responses in mice and it has been previously reported that intestinal tissues exhibit no toxicity with other high concentration CPPs (15–120 μ M) [26,66]. In conclusion, high-dose GET-based Insulin NCs can have significant effect on cell viability but monolayer integrity was maintained at lower doses, and barrier function was preserved. Future toxicity studies in mice will need to be conducted. Furthermore, the *in vitro* analyses could be extended by employing co-cultures of Caco-2 with mucus-secreting cells to assess penetration through this biofilm.

4.3. GET generates endosomal Insulin depots, which benefit chronic delivery and overall transcytosis

GET-peptide PLR (and its component peptides, P21, LK15, 8R) caused almost complete fluorescence quenching of Ins-F* at concentrations >1 μ M, while with individual component of GET system there was <50% quenching of fluorescence (Fig. 1). FITC is pH responsive, meaning that acidified endosomes could confound our analyses. We undertook control experiments in live as opposed to fixed cells, and showed that this was partly overcome, with the pH of endosomally localized Insulin likely to be equilibrated with fixation, and TRITC which is not pH responsive. Similar phenomenon of fluorescence quenching was reported for FITC-Insulin internalized by activated lymphocytes due to acidification, which was reversed using chloroquine, which mediates endosomal escape [67]. Our results agree with these studies, with brighter, uncomplexed, FITC-Insulin in cells treated with chloroquine due to endosomal escape (Fig. 6). Interestingly these studies also allowed the link between the Insulin depot hypothesis and these being, at least initially, defined as endosomes. High numbers of endosomes are progressively visualized perinuclearly with serial Insulin-GET NC deliveries. The brighter these cells are, the higher the transcytosis and secretion of subsequently delivered Insulin. The saturation of cells with Insulin therefore could be a mechanism by which Insulin may be steered away from endocytotic trapping and increased

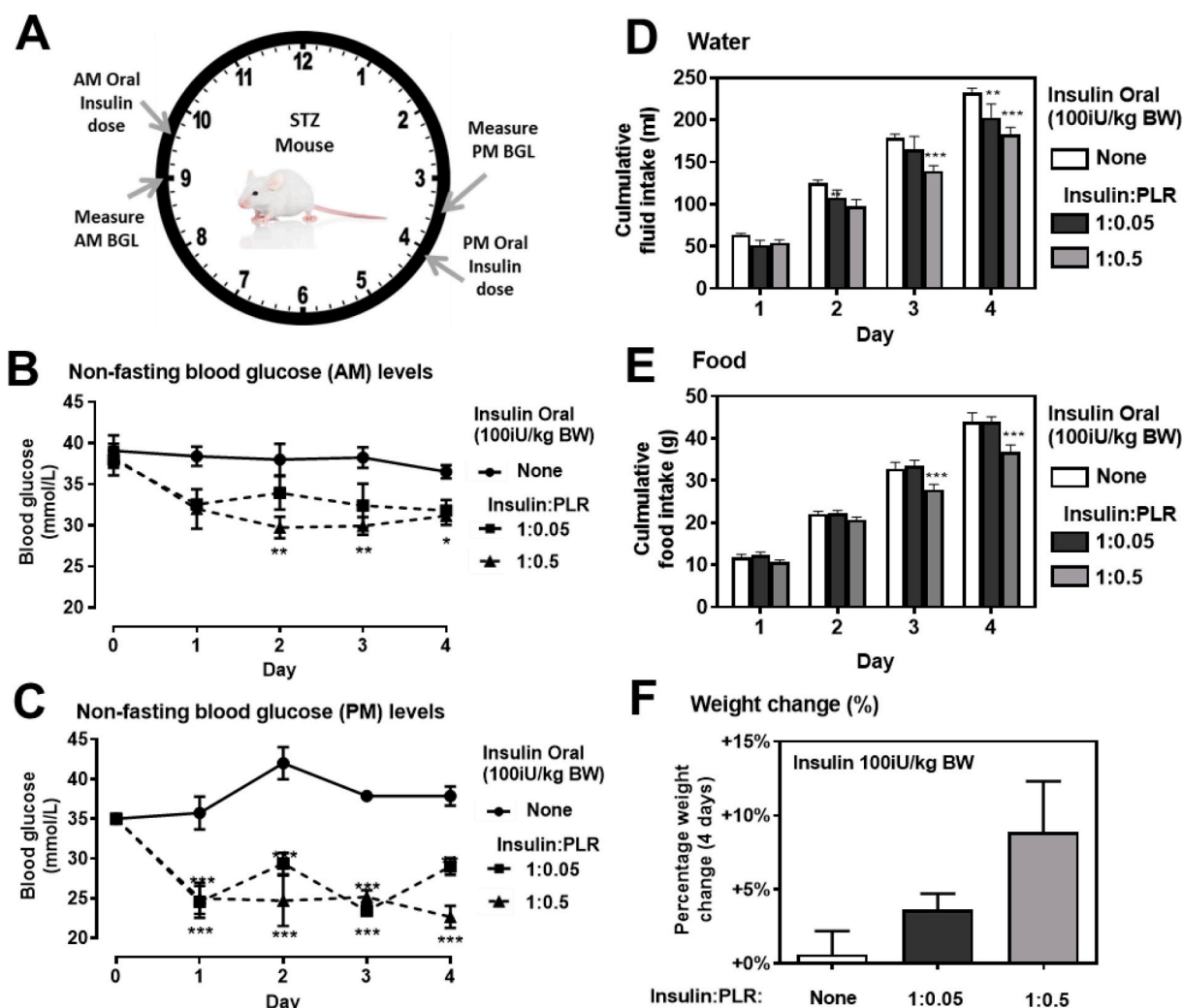


Fig. 9. Twice-daily oral Insulin delivery using GET stabilizes diabetic glycemia and improves body weight. **A.** Study animals were randomised based on non-fasting blood glucose which was measured at 9am and 3.30pm daily with assigned treatments administered 30 minutes later at both timepoints for 4 consecutive days, Treatments consisted of oral insulin alone, or in combination with GET ratios of 1:0.5 and 1:0.05 respectively. **B.** 9am blood glucose concentrations and 3.30pm (C) were measured and plotted over a 4-day period, results represent N=3/group SEM * $p < 0.05$, ** $p < 0.005$, *** $p < 0.0005$ via two-way ANOVA. **D.** Cumulative fluid and **E.** food intake was measured from each treatment animal. Results represent N=3/group SEM, ** $p < 0.005$, *** $p < 0.0005$ via two-way ANOVA. **F.** Body weight changes were tracked over the study duration and expressed at percentage change from baseline to day 4.

escape and release. It is interesting to note that the linkage between insulin and GET-peptide is non-covalent and that this electrostatic interaction can be cleaved by proteolytic enzymes, thereby releasing free Insulin to exert its pharmacological effects. However, a significant amount of Insulin that is successfully exocytosed is still complexed to GET (Fig. 5). This non-covalent interaction in Insulin-GET NCs was investigated for its stability using different assay based on the quenching phenomenon and cell lysate or collected media decomplexation with PK digestion. Interestingly, as anticipated GET stayed bound to Insulin (>60% from fluorescence recovery estimate) even after transcytosis, meaning that electrostatic interaction between Insulin and GET is stable enough to be delivered successfully across the cell monolayers. Surprisingly, cell internalized NCs were also stable and stayed intact while preserving NCs activity to the same extent as extracellular NCs. We conducted an experiment where successfully transcytosed and collected Insulin-GET NCs were re-delivered onto fresh monolayers. These samples again had enhanced uptake and release; with similar dynamics in new monolayers (enhanced cell retention), compared to saturated, multiply delivered monolayers (enhanced export). Therefore, it can be hypothesized that GET can protect Insulin and this could potentially transcytose through multiple cell layers to deliver intact Insulin into

systemic circulation without losing biological activity. The question arises of how Insulin escapes the GET peptide complex to mediate its biological function. Our data argues that as decomplexation is possible without proteolysis (with Heparin for example) and that Insulin-GET complexes have accessible Insulin (e.g., ELISA quantitation and biological function in complex) that Insulin may not need to fully escape the NCs on a molecular level. Further work would be useful to explore how receptor binding is mediated in complex with GET and if this facilitates local decomplexation to allow biological activity.

4.4. Loading and maintenance of Insulin uptake as a long-term route for oral insulin delivery

Multiple incubations/transductions are commonly being employed for numerous viral and non-viral genetic modification approaches in an attempt to attain improved transfection efficiency and prolonged gene expression [68,69]. Here, we assessed Insulin recycling in the context of multiple dosing using our transwell system. We observed that subsequent Insulin delivery in pre-tested cells tends to decrease the export of preloaded insulin out of the cells with increased exocytosis of the newly delivered Insulin. This phenomenon agrees with the general principal of

osmosis, meaning that saturating cells facilitates the success of future transcytosis.

Sustained release from cells loaded with Insulin using GET from our initial observations gave insight into recycling with cells acting as depots for sustained release. These results are in concordance with the previous studies, where CPPs have increased the intestinal absorption of Insulin [26,40,61,62] but when compared to that of octa-arginine (8R), GET allows cells to accumulate much more significant levels of Insulin to the extreme that their import overwhelms export and delivered cells become depotized. When cells are loaded with Insulin to this level subsequent, newly delivered Insulin, is less likely to be retained and more likely to be released. A loading and a maintenance dose for Insulin is an interesting concept when applied to oral delivery. In this case, we have serial oral delivery data showing that BGL can be maintained with twice-daily gavages. It is tempting to hypothesize that this is the first demonstration of a workable therapeutic dosing strategy that could be clinically viable. The large dose of Insulin used to regulate BGL (20iU/kg) is at least 5-fold more than that injected, however the response and duration of activity compared to an injected dose is extended and more controlled than bolus injection. It could be possible that such a dose could be scaled to clinical trial, however marrying the Insulin-GET NC system with controlled or enteric-coated systems could bring doses and bioavailability into a translatable range.

4.5. Future directions to enhance GET delivery of oral insulin

Very recently Oramed's oral Insulin trial (ORA-D-013-1) failed to meet its primary endpoint in improving glycaemic control in T2DM patients [70]. This again reiterates that new approaches are required if we are to reinvigorate the field in generating oral Insulin translation. Use of CPPs to deliver Insulin is not a new concept [20–25] with progressive refinements, for example penetratin and its analogues (shuffle & penetramax) have demonstrated superior performance *in vitro* and *in vivo* for promoting transmucosal delivery of insulin following oral administration [71–75]. However, it is notable that no CPP strategy has made it to the clinical trials despite 20 years of development. Although we have employed Insulin in great excess, there have been no studies that have shown the BGL levelling capacity of Insulin with a CPP as we demonstrate here. Several studies that have increased Insulin bioavailability *in vivo* highlight the importance of utilizing protease-resistant D-isomer peptide variants as a predominant strategy to overcome proteolytic sensitivity of the system in oral applications [25]. D-peptides exhibit extended half-lives *in vivo* compared to L-isomer peptides. Moreover, cellular uptake of CPPs is independent of chirality of peptide backbone [76,77] with D-arginine-rich CPPs being less susceptible to proteolytic degradation with a high affinity for serum proteins and provided greater intracellular delivery compared to its counterpart L-form [78]. Future generation of D-isoforms of GET (D-PLR) will now be tested, compared to the corresponding L-form (L-PLR). It was noteworthy that although NC formation did inhibit Insulin biological activity, a significant amount was retained by their direct ability to induce insulin-reporter cells (Fig. 7) and effect on BGL in the optimal formulation. Data would argue there is a trade-off between complexation with PLR and availability to interact with and activate receptors, which is highly influenced by GET concentration. Thus, suggesting that Insulin interaction with GET if at the correct dosing does not prevent Insulin's functional activity, as it is still pharmacologically active to exert biological effect, but also facilitates oral delivery, with successful BGL control. Whether stability of the GET peptide itself is inhibitory for this will need to be determined in future experiments in wild-type animals (pharmacokinetic data) and in diabetic animals. Experiments were conducted in fasted (Fig. 8) and fed (Fig. 9) mice. The magnitude of BGL lowering activity in these contexts should also be examined in detail in respect to residence time in the gut and the influence of gastric emptying on efficacy. Fasted and fed states could also generate counter-regulatory responses that act to further lower BGL, such as increased glucagon

secretion which need investigation.

Importantly we have demonstrated that without complex encapsulation or enteric-coating strategies, that a CPP-based approach and the use of simple electrostatic complexation can be a viable strategy for orally effective BGL control.

5. Conclusion

In recent years, one of the greatest challenges to oral Insulin delivery has been identified which is to overcome the intestinal epithelial and mucosal barrier. Non-viral vectors offer advantage due to their ease of modification for navigating extracellular barriers, targeting specific ligands on cell membrane, and to attain improved intracellular trafficking of therapeutic cargoes. In this study, we have described a simple and robust method to fabricate Insulin-GET NCs using non-covalent (electrostatic) approach, the generated NCs provided significantly enhanced absorption, permeation, transcytosis, and internalization of Insulin across *in vitro* intestinal Caco-2 cell monolayers, thereby suggesting that this system could be possibly employed for improving the oral delivery of Insulin. Insulin-GET NCs retained stability and accumulated in cells with progressive intracellular localization of vesicular Insulin promoting newly internalized Insulin to be released, with transcytosis enhanced. GET-based Insulin NCs retain functional activity and recycled NCs can re-transcytose if exposed to new cells. Single doses reduced BGL in diabetic animals to normoglycemic levels and twice-daily delivery robustly lowered glucose levels of these animals demonstrating a successful oral strategy. We believe that our system will serve as a powerful tool for overcoming the barriers of low permeability of Insulin and other anti-diabetic peptides as a model, such as stable Incretin mimetics [79–82], and the potential to be translated into a patient-applicable technology.

Author contributions

J.E.D. conceived and initiated the project; S.R., C.M. M., R. C.M., P.R. F. and J.E.D. designed the experiments; S.R., C.M.M., H.M.E, R.C.M. and J.E.D. conducted the experiments; P.R.F. and J.E.D. supervised the study; S.R., P.R.F. and J.E.D. wrote the manuscript; All authors approved the final manuscript.

CRediT authorship contribution statement

Sahrish Rehmani: Conceptualization, Data curation, Formal analysis, Investigation, Methodology, Validation, Writing – original draft, Writing – review & editing. **Christopher M. McLaughlin:** Data curation, Formal analysis, Investigation, Methodology, Validation, Visualization, Writing – original draft. **Hoda M. Eltahir:** Data curation, Formal analysis, Investigation, Methodology, Validation, Visualization. **R. Charlotte Moffett:** Data curation, Formal analysis, Investigation, Methodology, Validation, Visualization. **Peter R. Flatt:** Conceptualization, Funding acquisition, Project administration, Resources, Supervision, Writing – original draft, Writing – review & editing. **James E. Dixon:** Conceptualization, Formal analysis, Funding acquisition, Investigation, Project administration, Resources, Supervision, Validation, Writing – original draft, Writing – review & editing.

Declaration of Competing Interest

The authors declare no conflict of interest.

Data availability

Data will be made available on request.

Acknowledgements

The research leading to these results has received funding from the European Research Council under the European Community's Seventh Framework Programme (FP7/2007-2013)/ERC grant agreement 227845 and strategic research funding by Ulster University. J.E.D acknowledges the support of the Medical Research Council, the Engineering and Physical Sciences Research Council, and the Biotechnology and Biological Sciences Research Council UK Regenerative Medicine Platform Hub "Acellular Approaches for Therapeutic Delivery" (MR/K026682/1). R.C.M. is recipient of an R.D. Lawrence Fellowship of Diabetes UK. S.R acknowledges the support of Punjab Educational Endowment Fund (PEEF) scholarship, Government of Punjab, Pakistan. We thank David Onion and team at the Flow cytometry facility (University of Nottingham) for expertise in flow cytometry and ImageStream analyses.

Appendix A. Supplementary data

Supplementary data to this article can be found online at <https://doi.org/10.1016/j.jconrel.2023.06.006>.

References

- [1] A. Bolhassani, B.S. Jafarzade, G. Mardani, In vitro and in vivo delivery of therapeutic proteins using cell penetrating peptides, *Peptides* 87 (2017) 50–63.
- [2] C.O. Weill, S. Biri, A. Adib, P. Erbacher, A practical approach for intracellular protein delivery, *Cytotechnology* 56 (2008) 41–48.
- [3] N. Easa, R. Alany, M. Carew, A. Vangala, A review of non-invasive insulin delivery systems for diabetes therapy in clinical trials over the past decade, *Drug Discov. Today* 24 (2) (2019) 440–451, <https://doi.org/10.1016/j.drudis.2018.11.010>. Epub 2018 Nov 19.
- [4] E. Moroz, S. Matoori, J.-C. Leroux, Oral delivery of macromolecular drugs: where we are after almost 100 years of attempts, *Adv. Drug Deliv. Rev.* 101 (2016) 108–121.
- [5] M. Gallo, S. Defaus, D. Andreu, 1988–2018: Thirty years of drug smuggling at the nano scale. Challenges and opportunities of cell-penetrating peptides in biomedical research, *Archives of biochemistry and biophysics*, 2018.
- [6] H.A.-D.M. Abu-Awwad, L. Thiagarajan, J.M. Kanczler, M.H. Amer, G. Bruce, S. Lanham, R.M.H. Rumney, R.O.C. Oreffo, J.E. Dixon, Genetically-programmed, mesenchymal stromal cell-laden & mechanically strong 3D bioprinted scaffolds for bone repair, *J. Control. Release* 325 (2020) 335–346.
- [7] H.A.-D.M. Abu-Awwad, L. Thiagarajan, J.E. Dixon, Controlled release of GAG-binding enhanced transduction (GET) peptides for sustained and highly efficient intracellular delivery, *Acta Biomater.* 57 (2017) 225–237.
- [8] L.A. Blokpoel Ferreras, S.Y. Chan, S. Vazquez Reina, J.E. Dixon, Rapidly transducing and spatially localized magnetofection using peptide-mediated non-viral gene delivery based on iron oxide nanoparticles, *ACS Appl. Nano Mater.* 4 (2020) 167–181.
- [9] L.A. Blokpoel Ferreras, D. Scott, S. Vazquez Reina, P. Roach, T.E. Torres, G.F. Goya, K.M. Shakesheff, J.E. Dixon, Enhanced Cellular Transduction of Nanoparticles Resistant to Rapidly Forming Plasma Protein Coronas 4, 2020, p. 2000162.
- [10] J.E. Dixon, G. Osman, G.E. Morris, H. Markides, M. Rotherham, Z. Bayoussief, A. J. El Haj, C. Denning, K.M. Shakesheff, Highly efficient delivery of functional cargoes by the synergistic effect of GAG binding motifs and cell-penetrating peptides, *Proc. Natl. Acad. Sci.* 113 (2016) E291–E299.
- [11] H.M. Eltaher, L.A. Blokpoel Ferreras, A.R. Jalal, J.E. Dixon, Direct contact-mediated non-viral gene therapy using thermo-sensitive hydrogel-coated dressings, *Biomater. Adv.* 143 (2022), 213177.
- [12] H.M. Eltaher, J. Yang, K.M. Shakesheff, J.E. Dixon, Highly efficient intracellular transduction in three-dimensional gradients for programming cell fate, *Acta Biomater.* 41 (2016) 181–192.
- [13] A.R. Jalal, J.E. Dixon, Efficient delivery of transducing polymer nanoparticles for gene-mediated induction of osteogenesis for bone regeneration, *Front. Bioeng. Biotechnol.* 8 (2020) 849.
- [14] H. Markides, K.J. Newell, H. Rudolf, L.B. Ferreras, J.E. Dixon, R.H. Morris, M. Graves, J. Kaggie, F. Henson, A.J. El Haj, Ex vivo MRI cell tracking of autologous mesenchymal stromal cells in an ovine osteochondral defect model, *Stem Cell Res Ther* 10 (2019) 25.
- [15] G. Osman, J. Rodriguez, S.Y. Chan, J. Chisholm, G. Duncan, N. Kim, A.L. Tatler, K. M. Shakesheff, J. Hanes, J.S. Suk, PEGylated enhanced cell penetrating peptide nanoparticles for lung gene therapy, *J. Control. Release* 285 (2018) 35–45.
- [16] R.N. Power, B.L. Cavanagh, J.E. Dixon, C.M. Curtin, F.J. O'Brien, Development of a gene-activated scaffold incorporating multifunctional cell-penetrating peptides for pSDF-1 α , *Deliv. Enhanc. Angiogenesis. Tissue Eng. Appl.* 23 (2022) 1460.
- [17] R.M. Raftery, D.P. Walsh, L. Blokpoel Ferreras, I. Mencía Castaño, G. Chen, M. LeMoine, G. Osman, K.M. Shakesheff, J.E. Dixon, F.J. O'Brien, Highly versatile cell-penetrating peptide loaded scaffold for efficient and localised gene delivery to multiple cell types: from development to application in tissue engineering, *Biomaterials* 216 (2019), 119277.
- [18] R.M.H. Rumney, S.A. Lanham, J.M. Kanczler, A.P. Kao, L. Thiagarajan, J.E. Dixon, G. Tozzi, R.O.C. Oreffo, In vivo delivery of VEGF RNA and protein to increase osteogenesis and intrasosseous angiogenesis, *Sci. Rep.* 9 (2019) 17745.
- [19] A. Spiliotopoulos, L. Blokpoel Ferreras, R.M. Densham, S.G. Caulton, B. C. Maddison, J.R. Morris, J.E. Dixon, K.C. Gough, I. Dreveny, Discovery of peptide ligands targeting a specific ubiquitin-like domain's binding site in the deubiquitinase USP11, *J. Biol. Chem.* 294 (2019) 424–436.
- [20] S. Gao, M.J. Simon, C.D. Hue, B. Morrison III, S. Banta, An unusual cell penetrating peptide identified using a plasmid display-based functional selection platform, *ACS Chem. Biol.* 6 (2011) 484–491.
- [21] S. Pujals, E. Sabidó, T. Tarragó, E., Giralt, all-D Proline-Rich Cell-Penetrating Peptides: A Preliminary In Vivo Internalization Study, in, Portland Press Ltd., 2007.
- [22] F. Salomone, F. Cardarelli, M. Di Luca, C. Boccardi, R. Nifosi, G. Bardi, L. Di Bari, M. Serresi, F. Beltram, A novel chimeric cell-penetrating peptide with membrane-disruptive properties for efficient endosomal escape, *J. Control. Release* 163 (2012) 293–303.
- [23] A. Sharma, A.A. Pohane, S. Bansal, A. Bajaj, V. Jain, A. Srivastava, Cell penetrating synthetic antimicrobial peptides (SAMPs) exhibiting potent and selective killing of *Mycobacterium* by targeting its DNA, *Chem Eur J* 21 (2015) 3540–3545.
- [24] N.-Q. Shi, X.-R. Qi, B. Xiang, Y. Zhang, A survey on "Trojan horse" peptides: opportunities, issues and controlled entry to "Troy", *J. Control. Release* 194 (2014) 53–70.
- [25] W.P. Verdurmen, P.H. Bovee-Geurts, P. Wadhvani, A.S. Ulrich, M. Hällbrink, T. H. van Kuppevelt, R. Brock, Preferential uptake of L-versus D-amino acid cell-penetrating peptides in a cell type-dependent manner, *Chem. Biol.* 18 (2011) 1000–1010.
- [26] N. Kamei, E.J.B. Nielsen, E.-S. Khafagy, M. Takeda-Morishita, Noninvasive insulin delivery: the great potential of cell-penetrating peptides, *Ther. Deliv.* 4 (2013) 315–326.
- [27] N. Kamei, Y. Onuki, K. Takayama, M. Takeda-Morishita, Mechanistic study of the uptake/permeation of cell-penetrating peptides across a caco-2 monolayer and their stimulatory effect on epithelial insulin transport, *J. Pharm. Sci.* 102 (2013) 3998–4008.
- [28] S. Higashiyama, J.A. Abraham, M. Klagsbrun, Heparin-binding EGF-like growth factor stimulation of smooth muscle cell migration: dependence on interactions with cell surface heparan sulfate, *J. Cell Biol.* 122 (1993) 933–940.
- [29] E. Koren, V.P. Torchilin, Cell-penetrating peptides: breaking through to the other side, *Trends Mol. Med.* 18 (2012) 385–393.
- [30] S. Rehmani, J.E. Dixon, Oral delivery of anti-diabetes therapeutics using cell penetrating and transcytosing peptide strategies, *Peptides* 100 (2018) 24–35.
- [31] J.B. Rothbard, T.C. Jessop, R.S. Lewis, B.A. Murray, P.A. Wender, Role of membrane potential and hydrogen bonding in the mechanism of translocation of guanidinium-rich peptides into cells, *J. Am. Chem. Soc.* 126 (2004) 9506–9507.
- [32] V.A. Gault, N. Irwin, P. Harriott, P.R. Flatt, F.P.M. O'Harte, DPP IV resistance and insulin releasing activity of a novel di-substituted analogue of glucose-dependent insulinotropic polypeptide, (Ser2-Asp13)GIP, *Cell Biol. Int.* 27 (2003) 41–46.
- [33] R. Othman, G.E. Morris, D. Shah, S. Hall, G. Hall, K.B. Wells, K.M. Shakesheff, J.E. Dixon, An automated fabrication strategy to create patterned tubular architectures at cell and tissue scales 7, 2015.
- [34] H.M. Eltaher, F.E. Abukunna, L. Ruiz-Cantu, Z. Stone, J. Yang, J.E. Dixon, Human-scale tissues with patterned vascular networks by additive manufacturing of sacrificial sugar-protein composites, *Acta Biomater.* 113 (2020) 339–349.
- [35] L. Thiagarajan, H.A.-D.M. Abu-Awwad, J.E. Dixon, Osteogenic programming of human mesenchymal stem cells with highly efficient intracellular delivery of RUNX2, *Stem Cells Transl. Med.* 6 (2017) 2146–2159.
- [36] C.M. McLaughlin, S.J. Sharkey, P. Harnedy-Rothwell, V. Parthasarathy, P.J. Allsopp, E.M. McSorley, R.J. FitzGerald, F.P.M. O'Harte, Twice daily oral administration of *Palmaria palmata* protein hydrolysate reduces food intake in streptozotocin induced diabetic mice, improving glycaemic control and lipid profiles, *J. Funct. Foods* 73 (2020), 104101.
- [37] N. Kamei, M. Morishita, K. Takayama, Importance of intermolecular interaction on the improvement of intestinal therapeutic peptide/protein absorption using cell-penetrating peptides, *J. Control. Release* 136 (2009) 179–186.
- [38] M. Kristensen, H. Franzyk, M.T. Klausen, A. Iversen, J.S. Bohnsen, R. B. Skyggebjerg, V. Foderà, H.M. Nielsen, Penetratin-mediated transepithelial insulin permeation: importance of cationic residues and pH for complexation and permeation, *AAPS J.* 17 (2015) 1200–1209.
- [39] M. Kristensen, H.M. Nielsen, Cell-penetrating peptides as carriers for Oral delivery of biopharmaceuticals, *Basic Clin. Pharmacol. Toxicol.* 118 (2016) 99–106.
- [40] M. Morishita, N. Kamei, J. Ehara, K. Isowa, K. Takayama, A novel approach using functional peptides for efficient intestinal absorption of insulin, *J. Control. Release* 118 (2007) 177–184.
- [41] Z. Oren, J.C. Lerman, G.H. Gudmundsson, B. Agerberth, Y. Shai, Structure and organization of the human antimicrobial peptide LL-37 in phospholipid membranes: relevance to the molecular basis for its non-cell-selective activity, *Biochem. J.* 341 (1999) 501.
- [42] S. Kwon, J.H. Carson, Fluorescence quenching and Dequenching analysis of RNA Interactions *In Vitro* and *In Vivo*, *Anal. Biochem.* 264 (1998) 133–140.
- [43] J.-H. Wu, S.L. Diamond, A fluorescence quench and dequench assay of fibrinogen polymerization, fibrinogenolysis, or fibrinolysis, *Anal. Biochem.* 224 (1995) 83–91.
- [44] A. Fedi, C. Vitale, G. Ponschin, S. Ayeuhunie, M. Fato, S. Scaglione, In vitro models replicating the human intestinal epithelium for absorption and metabolism studies: a systematic review, *J. Control. Release* 335 (2021) 247–268.

- [45] V. Meunier, M. Bourrié, Y. Berger, G. Fabre, The human intestinal epithelial cell line Caco-2; pharmacological and pharmacokinetic applications, *Cell Biol. Toxicol.* 11 (1995) 187–194.
- [46] M. Arslanti, M. Lim, C.P. Marquis, R. Amal, Polyethylenimine based magnetic Iron-oxide vector: the effect of vector component assembly on cellular entry mechanism, intracellular localization, and cellular viability, *Biomacromolecules* 11 (2010) 2521–2531.
- [47] J.S. Wadia, R.V. Stan, S.F. Dowdy, Transducible TAT-HA fusogenic peptide enhances escape of TAT-fusion proteins after lipid raft macropinocytosis, *Nat. Med.* 10 (2004) 310–315.
- [48] W. Shan, X. Zhu, M. Liu, L. Li, J. Zhong, W. Sun, Z. Zhang, Y. Huang, Overcoming the diffusion barrier of mucus and absorption barrier of epithelium by self-assembled nanoparticles for oral delivery of insulin, *ACS Nano* 9 (2015) 2345–2356.
- [49] J.E. Heuser, R.G. Anderson, Hypertonic media inhibit receptor-mediated endocytosis by blocking clathrin-coated pit formation, *J. Cell Biol.* 108 (1989) 389–400.
- [50] I.S. Zuhorn, R. Kalicharan, D. Hoekstra, Lipoplex-mediated transfection of mammalian cells occurs through the cholesterol-dependent clathrin-mediated pathway of endocytosis, *J. Biol. Chem.* 277 (2002) 18021–18028.
- [51] A.K. Varkouhi, M. Scholte, G. Storm, H.J. Haisma, Endosomal escape pathways for delivery of biologicals, *J. Control. Release* 151 (2011) 220–228.
- [52] S. Seino, Cell signalling in insulin secretion: the molecular targets of ATP, cAMP and sulfonylurea, *Diabetologia* 55 (2012) 2096–2108.
- [53] D.P. Kumar, S. Rajagopal, S. Mahavadi, F. Mirshahi, J.R. Grider, K.S. Murthy, A. J. Sanyal, Activation of transmembrane bile acid receptor TGR5 stimulates insulin secretion in pancreatic β cells, *Biochem. Biophys. Res. Commun.* 427 (2012) 600–605.
- [54] Y. Zhao, Q. Fang, S.G. Straub, M. Lindau, G.W. Sharp, Hormonal inhibition of endocytosis: novel roles for noradrenaline and G protein Gz, *J. Physiol.* 588 (2010) 3499–3509.
- [55] Y. Zhao, Q. Fang, S.G. Straub, M. Lindau, G.W. Sharp, Noradrenaline inhibits exocytosis via the G protein $\beta\gamma$ subunit and refilling of the readily releasable granule pool via the $\alpha 1/2$ subunit, *J. Physiol.* 588 (2010) 3485–3498.
- [56] T. Nakaki, T. Nakadate, R. Kato, Alpha 2-adrenoceptors modulating insulin release from isolated pancreatic islets, *Naunyn Schmiedeberg's Arch. Pharmacol.* 313 (1980) 151–153.
- [57] D.E. Wiedenkel, G.W.G. Sharp, Effects of forskolin on insulin release and cyclic amp content in rat pancreatic islets, *Endocrinology* 113 (1983) 2311–2313.
- [58] M. Boushra, S. Tous, G. Fetih, H.-Y. Xue, H.-L. Wong, Development of bi-polymer lipid hybrid nanocarrier (BLN) to improve the entrapment and stability of insulin for efficient oral delivery, *J. Drug Deliv. Sci. Technol.* 49 (2019) 632–641.
- [59] N. Svensen, J.G. Walton, M. Bradley, Peptides for cell-selective drug delivery, *Trends Pharmacol. Sci.* 33 (2012) 186–192.
- [60] I.A. Khalil, K. Kogure, S. Futaki, H. Harashima, High density of octaarginine stimulates macropinocytosis leading to efficient intracellular trafficking for gene expression, *J. Biol. Chem.* 281 (2006) 3544–3551.
- [61] J.F. Liang, V.C. Yang, Insulin-cell penetrating peptide hybrids with improved intestinal absorption efficiency, *Biochem. Biophys. Res. Commun.* 335 (2005) 734–738.
- [62] N. Kamei, M. Morishita, Y. Eda, N. Ida, R. Nishio, K. Takayama, Usefulness of cell-penetrating peptides to improve intestinal insulin absorption, *J. Control. Release* 132 (2008) 21–25.
- [63] L.N. Patel, J. Wang, K.-J. Kim, Z. Borok, E.D. Crandall, W.-C. Shen, Conjugation with cationic cell-penetrating peptide increases pulmonary absorption of insulin, *Mol. Pharm.* 6 (2009) 492–503.
- [64] A. Tavernier, R. Dondi, K. Almansour, F. Laurent, S.-E. Owens, I.M. Eggleston, N. Fotaki, R.J. Mrsny, Enhanced paracellular transport of insulin can be achieved via transient induction of myosin light chain phosphorylation, *J. Control. Release* 210 (2015) 189–197.
- [65] N. Kamei, H. Tamiwa, M. Miyata, Y. Haruna, K. Matsumura, H. Ogino, S. Hirano, K. Higashiyama, M. Takeda-Morishita, Hydrophobic amino acid tryptophan shows promise as a potential absorption enhancer for oral delivery of biopharmaceuticals, *Pharmaceutics* 10 (2018) 182.
- [66] Z. Niu, E. Samaridou, E. Jaumain, J. Coëne, G. Ullio, N. Shrestha, J. Garcia, M. Durán-Lobato, S. Tovar, M.J. Santander-Ortega, PEG-PGA enveloped octaarginine-peptide nanocomplexes: an oral peptide delivery strategy, *J. Control. Release* 276 (2018) 125–139.
- [67] R.F. Murphy, E. Bisaccia, C.R. Cantor, C. Berger, R.L. Edelson, Internalization and acidification of insulin by activated human lymphocytes, *J. Cell. Physiol.* 121 (1984) 351–356.
- [68] S. McLenachan, D. Zhang, A.B.A. Palomo, M.J. Edel, F.K. Chen, mRNA transfection of mouse and human neural stem cell cultures, *PLoS One* 8 (2013), e83596.
- [69] M. Yamamoto, S. Okumura, C. Schwencke, J. Sadoshima, Y. Ishikawa, High efficiency gene transfer by multiple transfection protocol, *Histochem. J.* 31 (1999) 241–243.
- [70] O. Ltd, Study to Evaluate the Efficacy and Safety of ORMD-0801 in Subjects with Type 2 Diabetes Mellitus, in: *Clinical Trials FDA*, 2023.
- [71] R.G. Diedrichsen, S. Harloff-Helleberg, U. Werner, M. Besenius, E. Leberer, M. Kristensen, H.M. Nielsen, Revealing the importance of carrier-cargo association in delivery of insulin and lipidated insulin, *J. Control. Release* 338 (2021) 8–21.
- [72] N. Kamei, S. Kawano, R. Abe, S. Hirano, H. Ogino, H. Tamiwa, M. Takeda-Morishita, Effects of intestinal luminal contents and the importance of microfold cells on the ability of cell-penetrating peptides to enhance epithelial permeation of insulin, *Eur. J. Pharm. Biopharm.* 155 (2020) 77–87.
- [73] M. Kristensen, R. Guldsmed Diedrichsen, V. Vetri, V. Foderà, H. Mørck Nielsen, Increased Carrier Peptide Stability through pH Adjustment Improves Insulin and PTH(1–34) Delivery in Vitro and in Vivo Rather than by Enforced Carrier Peptide-Cargo Complexation, *Pharmaceutics*, 12, 2020.
- [74] B.B. Alsulaym, M.K. Anwer, G.A. Soliman, S.M. Alshehri, E.S. Khafagy, Impact of penetratin stereochemistry on the oral bioavailability of insulin-loaded solid lipid nanoparticles, *Int. J. Nanomedicine* 14 (2019) 9127–9138.
- [75] R.G. Diedrichsen, P.S. Tuelung, V. Foderà, H.M. Nielsen, Stereochemistry and intermolecular interactions influence carrier peptide-mediated insulin delivery, *Mol. Pharm.* 20 (2023) 1202–1212.
- [76] D. Derossi, S. Calvet, A. Trembleau, A. Brunissen, G. Chassaing, A. Prochiantz, Cell internalization of the third helix of the Antennapedia homeodomain is receptor-independent, *J. Biol. Chem.* 271 (1996) 18188–18193.
- [77] J. Brugidou, C. Legrand, J. Mery, A. Rabie, The retro-inverso form of a homeobox-derived short peptide is rapidly internalized by cultured neurons: a new basis for an efficient intracellular delivery system, *Biochem. Biophys. Res. Commun.* 214 (1995) 685–693.
- [78] I. Nakase, Y. Konishi, M. Ueda, H. Saji, S. Futaki, Accumulation of arginine-rich cell-penetrating peptides in tumors and the potential for anticancer drug delivery in vivo, *J. Control. Release* 159 (2012) 181–188.
- [79] G.V. Graham, C.M. McLaughlin, P.R. Flatt, Role of exendin-4 in the Gila monster: further lessons regarding human oral glucagon-like peptide-1 therapy? *Diabetes Obes. Metab.* 22 (2020) 2509–2511.
- [80] F.G. Eliashchewitz, L.H. Canani, Advances in GLP-1 treatment: focus on oral semaglutide, *Diabetol. Metab. Syndr.* 13 (2021) 99.
- [81] C. Brincat, Researchers identify insulin-mimicking molecule that could treat diabetes, in: J.S. Schulman (Ed.), *Medical News Today*, 2023. Available at: <https://www.medicalnewstoday.com/articles/diabetes-insulin-mimicking-molecule-could-be-developed-into-oral-pill>.
- [82] N.S. Kirk, Q. Chen, Y.G. Wu, A.L. Asante, H. Hu, J.F. Espinosa, F. Martínez-Olíd, M. B. Margetts, F.A. Mohammed, V.V. Kiselyov, D.G. Barrett, M.C. Lawrence, Activation of the human insulin receptor by non-insulin-related peptides, *Nat. Commun.* 13 (2022) 5695.